Received: 30 June 2020 | Revised: 3 December 2020 | Accepted: 25 January 2021

DOI: 10.1002/kin.21483

INTERNATIONAL JOURNAL OF CHEMICAL KINETICS WILEY

ARTICLE

An experimental and kinetic modeling study of the ignition delay and heat release characteristics of a five component gasoline surrogate and its blends with iso-butanol within a rapid compression machine

Christian Michelbach | **Alison Tomlin**

School of Chemical and Process Engineering, University of Leeds, Leeds, UK

Correspondence
Christian Michelbach, School of Chemical and Process Engineering, University of Leeds, Leeds LS2 9JT, UK.
Email: c.michelbach@leeds.ac.uk

Abstract

This study investigates the performance of a five component gasoline surrogate (iso-octane, toluene, *n*-heptane, 1-hexene, and ethanol) in representing the ignition delay time (IDT) behavior of gasoline (reference gasoline PR5801—research octane number 95.4, motor octane number 86.6), at conditions of 675–870 K, 20 bar, and $\Phi = 1$ (stoichiometric) within a rapid compression machine (RCM). Experimentally, the surrogate produces a good representation of the ignition behavior of the gasoline at these conditions, displaying a similar IDT profile. The influence of blending with iso-butanol on the surrogate's ignition delay behavior is also investigated, at blends from 5% to 70% of iso-butanol by volume. The surrogate continues to produce a reasonable representation of the experimental IDTs of gasoline and iso-butanol blends, except under a high degree of iso-butanol blending (50% iso-butanol), where the surrogate produced longer IDTs, particularly at temperatures below 740 K. Blends of 5% and 10% iso-butanol produce IDTs shorter than that of any other blend, including the "neat" surrogate, at temperatures of 740–770 and 830 K, respectively. Kinetic modeling of RCM IDTs is performed using CHEMKIN-PRO (Reaction Design: San Diego, CA, 2011) and a combined mechanism of the Sarathy et al. butanol isomers mechanism (*Progress in Energy and Combustion Science* 2014; 44: 40–102) and Lawrence Livermore National Laboratories "Gasoline Surrogate" mechanism (*Proceedings of the Combustion Institute* 2011; 33(1): 193–200). The model produces good IDT predictions below 740 K but overpredicts reactivity in the negative temperature coefficient region. Heat release rate analysis is conducted for experimental and modeling results to investigate low-temperature heat release (LTHR) behavior. Simulations largely fail to accurately reproduce this behavior. This analysis, combined with local OH and brute force Δh_f sensitivity analyses, indicates the significance of LTHR in the determination of IDTs and provides RCM heat release rates for future model validation.

KEYWORDS
butanol, gasoline surrogate, heat release, Ignition delay, sensitivity analysis

1 | INTRODUCTION

Bio-derived fuels, including bioalcohols, have emerged as attractive alternatives to fossil-derived fuels, either as single fuels or as blending components. Strategies for the limitation of climate change impacts mandate the reduction of transport emissions, including the use of a wide range of fossil fuel alternatives and supplements. The attractiveness of alcohols in this case is due in part to the physical and thermodynamic similarities they share with conventional fossil fuels, such as gasoline. This allows for possible applications in spark-ignition (SI) engine technologies and fuel distribution infrastructure with little to no modification.[1,2] It is common for ethanol to be used in such a way, blended in low amounts with gasoline before reaching the end consumer. The supplementation of gasoline with ethanol does not only carry potential greenhouse gas emissions benefits, but also a higher laminar burning velocity and potential knock resistance improvements.[1,3] Recently, longer chain bio-derived alcohols have been the subject of extensive research as a further alternative fuel/supplement, including the butanol isomers. When compared to ethanol, butanol is not hydrophilic, has a lower vapor pressure, lower degree of corrosivity, and higher calorific value. Butanol can also be produced as a "second-generation" biofuel, leading to a reduced impact on food crops, with production pathways identified for the *n*-, sec-, and iso-butanol isomers.[4,5] Of these, iso-butanol has been identified as the bioderivable isomer which provides the greatest knock-resistant ignition properties over a range of reasonable conditions.[6] The ignition characteristics of iso-butanol as a single component have been investigated in previous works.[6–8] However, it is vital to also fully understand the ignition characteristics of any alternative fuel or fuel supplement blend with gasoline, such that the feasibility of the fuel blending can be determined. The feasibility of a given blend is dependent on satisfying engine performance concerns, such as a fuel's knock resistance. This is not only important for use in current SI engines but also for emergent technologies such as turbo-charged, downsized engines, and homogeneous compression charge ignition (HCCI) engines.

The characterization of new fuels and blends, at engine-relevant conditions, can first be approached through fundamental combustion and ignition studies. These may elucidate fuel-dependent engine-relevant phenomena and provide insight into the underlying chemistry which drives the phenomena. The combustion properties of iso-butanol have been explored extensively in the literature due to a growing interest in its use as a renewably source biofuel for transport. Work by McEnally and Pfefferle[9] in 2005 marks the beginning of a growing interest in the combustion of butanol isomers and studied the decomposition and hydrocarbon growth process for each of them. Flame speciation measurements revealed that the butanol isomers produced much higher concentrations of ketone and aldehyde species than alkane dopants. However, the quantity of such toxic combustion products could be limited through the blending of butanol with gasoline, limiting the quantity of alcohol in the fuel. Grana et al.[10] continued this work, investigating the structure and speciation of non-premixed counterflow flames of iso-butanol and they developed a high-temperature kinetic mechanism for the combustion of butanol isomers. Laminar burning velocities for the butanol isomers and flame instabilities were investigated by Gu et al.[11] using butanol/air premixed spherically expanding flames. This study found that laminar burning velocities were generally greater for *n*-butanol, decreasing further in the order sec-butanol, iso-butanol, tert-butanol, with branching methyl groups decreasing the laminar burning velocity. The molecular structure had no apparent impact on the flame instability, however, with each of the butanol isomers displaying cellular structures at similar flame radii.[11] These findings were further supported by the work of Veloo and Egolfopoulos,[12] which showed the same order of flame speeds at an initial mixture temperature of 343 K, atmospheric pressure, and a wide range of equivalence ratios. This would suggest that, within engines, *n*-butanol and the associated blended fuels may produce higher power output than iso-butanol and its blends but also a greater propensity for knock, given the higher degree of autoignitive propensity of *n*-butanol. Detailed flame structures for the butanol isomers were measured using molecular beam mass spectrometry by Oßwald et al.[13] for laminar flat premixed low-pressure (40 mbar) flames, at $\Phi = 1.7$. This work showed that temperature and species measurements for the butanol isomers were strikingly similar, suggesting global combustion behavior between the isomers. The intermediate species pools, however, displayed significant variation, indicating fuel-specific pathways.[13] A further low-pressure premixed flame study by Hansen et al.[14] provided further speciation measurements of over 40 individual species for the butanol isomers. These flame studies provide important species measurements during combustion which can be used for the validation of kinetic mechanisms and reveal

important quantitative data on the production of aldehydes, enols, and alkenes during the combustion process.[1]

The autoignition behavior of "neat" butanol isomers has been the subject of much research; however, investigations focusing on blends of butanol with gasoline are scarce. Shock tube measurements of the butanol isomer ignition delay time (IDTs) are available in the literature, typically under high-temperature conditions (>1000 K).[7,8,15] Moss et al.[8] investigated the high-temperature autoignition behavior of the butanol isomers in a shock tube, at temperatures and pressures of 1200–1800 K and 1–4 bar, respectively. Under these conditions, the study determined that the isomers, in the order of decreasing reactivity, were *n*-butanol, iso-butanol, sec-butanol, and tert-butanol. This supports the findings at lower temperatures in the rapid compression machine (RCM),[6,16] which showed a similar ordering of reactivity, but with iso-butanol decreasing in reactivity relative to the other isomers as pressure increased, displaying the largest IDTs at a pressure of 30 bar. This indicates that, at the low temperature, high-pressure conditions characteristic of modern engine technologies (such as downsized pressure boosted SI engines), iso-butanol displays the greatest potential as a biofuel antiknocking agent when blended with gasoline. However, fundamental ignition studies which investigate this are scarce and the influence of iso-butanol blending on the antiknock properties of gasoline require a thorough characterization, particularly in the temperature and pressure regime of modern SI engine technologies. This would provide an insight into the behavior of such blends as well as an array of targets for model evaluation, creating the potential for model improvement in this highly important region.

Gasoline is a complex mixture of several hundred hydrocarbon species.[17] Due to the large amount and variety of hydrocarbons, the degree of complexity for a standard gasoline is too great to kinetically model precisely. Therefore, it is common practice to model the kinetics of gasolines using a less complex gasoline surrogate. These surrogates are designed to match characteristic properties of the reference gasoline, such that the surrogate's behavior in experiments is similar to that exhibited by the reference gasoline.[18] Traditionally, primary reference fuels (PRFs) were commonly utilized as gasoline surrogates for autoignition studies within shock tubes and RCMs.[19–21] These consist of a simple mixture of iso-octane and *n*-heptane, blended to match the motor octane number (MON) or research octane number (RON) of the reference gasoline. However, due to the small number of components, PRFs produce the same values for RON and MON, failing to represent the octane sensitivity of the reference gasoline. Through the addition of nonparaffinic components (such as olefins and aromatics), a three-component surrogate mixture can be determined which matches any target MON and RON values (and therefore octane sensitivity), typically through the addition of toluene to create a toluene reference fuel (TRF).[22] The capabilities of such fuels to match the autoignition behavior of gasolines have been evaluated in several previous studies.[23–29] However, when matching the properties of high octane sensitivity gasolines, TRF surrogates typically require toluene fractions greater than 30%, which does not accurately represent the hydrocarbon composition of gasoline fuels.[18] In these cases, additional surrogate components are required to match the octane properties of gasoline while maintaining a similar hydrocarbon distribution, including olefins,[30–33] naphthenes,[34–36] and (in the case of oxygenated reference gasolines) ethanol.[37–39] Recent studies have investigated the antiknock performance of an oxygenated RON 95 gasoline (and its surrogates), which is similar to that available to consumers in the European Union.[28,29,40,41] Agbro et al.[29] performed an RCM study on the influence of blending 20% *n*-butanol (by volume) with such a gasoline and found that, for compressed conditions of 678–858 K at 20 bar, *n*-butanol blending resulted in a lower degree of reactivity at low temperatures. However, as temperatures increased above 800 K, the addition of 20% *n*-butanol produced shorter IDTs. TRF and *n*-butanol blends replicated this behavior well. [29] Gorbatenko et al.[28] continued this work by extending the blending regime (10–85% *n*-butanol), and similarly found that, in general, the addition of *n*-butanol decreased reactivity at the low-temperature end of the investigated regime and increased reactivity in the high-temperature regime. However, their work showed significant discrepancies between the performance of the gasoline and TRF blends, particularly in the negative temperature coefficient (NTC) region and suggested that the addition of additional surrogate components was required to adequately represent the reference gasoline. [28] A thorough documentation of recent gasoline and surrogate literature is provided in the review of Sarathy et al.[18]

Alongside experimental investigations, several attempts have been made to produce chemical kinetic models which may predict the autoignition behavior of the butanol isomers,[10,42–45] as documented in the review of Sarathy et al.[1] Previous studies on the autoignition behavior of *n*-butanol blends with gasoline and its surrogate have identified considerable discrepancies between behavior observed in the RCM and model predictions, including IDTs and preliminary exothermicity, indicating the need for the further development of such models and an improvement in the understanding of the chemical kinetics of blended fuels.[28,29] Fundamental experiments, such as RCM IDT investigations, provide a range of validation targets for a model that are often relevant to real-world engine conditions. By providing the data from these

experiments, numerical models can be further analyzed, validated, and developed to increase their predictive ability at all relevant conditions. This is especially true for new fuels, which may have been exposed to little investigation and analysis. However, the validity of a given model is determined largely by the level of accuracy, or conversely uncertainties, of the underlying thermodynamic and kinetic data of each species and reaction. While some species and reactions are relatively well understood and as such have a low degree of associated uncertainty, much data (particularly for longer chain fuel radicals) is based on assumptions and estimates. Thermochemical properties, such as species enthalpy of formation, impact on energy balances and the position of chemical equilibria within a kinetic system. As such, these properties play an important role in the accurate prediction of ignition characteristics by chemical kinetic models. This importance results mostly from the direct impact of thermochemical properties on the determination of the equilibrium rate constant and the subsequent calculation of backward reaction rates. Where both forward and reverse rate constants are specified within a model, uncertainties in a species enthalpy of formation may have a negligible impact on global predictions. Therefore, analysis that investigates both reaction rate parameters and thermodynamic properties (namely enthalpy of formation) may provide a more substantial platform for model evaluation. Small species are often well characterized, either through experimental validation[46] or quantum chemical calculations[47] or through statistical optimization approaches incorporating combined sets of data.[48,49] However, in the case of thermodynamic data, estimates for larger species are often calculated via Benson's group additivity (GA),[50] which serves as an alternative and less resource-intensive method. Previous studies have investigated the impact of uncertainties in species thermodynamic data on the overall IDT, and they have been shown to produce a substantial overall uncertainty[51,52] in predicted outputs such as IDTs. This has also been shown to be the case for uncertainties in individual GA group values.[53] Therefore, it may be necessary to revisit fundamental estimated properties to produce a thoroughly robust and valid model.

Heat release analysis (HRA) is a tool which can be applied to both real RCM experimental data and simulated results, to further investigate a fuel's ignition behavior and the ability of a model to mimic this behavior. Due to an array of challenges concerning the use of RCM, such as significant heat losses, fuel transfer into piston crevices, and the difficulty in acquiring suitable transducer measurements, HRA has not traditionally been applied to RCM studies. However, recent studies have developed a method through which HRA may be applied to RCM experimental data.[54] This technique provides an avenue for significant further exploration of fuels and their ignition behavior, including the detection of inhomogeneous ignition events, the quantification of initial exothermicity, and the improvement of chemical kinetic knowledge and models.

Overall, studies of low-temperature autoignition of iso-butanol, at conditions relevant to modern SI engines, are scarce. As such, measurements taken in this region are valuable for developing a complete understanding of the fuel's autoignition behavior and as model validation targets. Such fundamental studies on the ignition and heat release behavior of iso-butanol and gasoline blends in this low temperature, high-pressure region appear to be largely absent from the literature. This blending regime requires thorough characterization, alongside equivalent studies of iso-butanol blends with a gasoline surrogate, that will facilitate the application of modeling and sensitivity analysis techniques in order to develop an understanding of the kinetic behavior driving changes to the ignition process due to blending. To meet this requirement, this study aims to investigate the autoignition of iso-butanol blends with gasoline and a surrogate at the fundamental level in an RCM, as well as to evaluate the ability of a newly developed gasoline surrogate to capture the ignition behavior of gasoline under blending. Computational modeling of the RCM, through the application of a detailed kinetic mechanism, will facilitate the further analysis of the influence of blending on the underlying chemistry driving autoignition phenomena.

2 | METHOD

2.1 | Gasoline surrogate

To match the needs of this study, a five-component surrogate (hereby referred to as 5-C) was produced. This surrogate has been designed to closely match the relevant properties of the PR5801 reference gasoline (supplied by Shell Global Solutions), specifically the RON and MON, hydrogen to carbon (H/C) ratio, and molecular composition. Chemical properties such as the RON, MON and H/C ratio are key to describing the autoignitive and antiknocking behavior of the gasoline, and as such should be matched as closely as possible by any given surrogate.

The molecular composition of the gasoline is responsible for the determination of all subsequent chemical and physical properties, such as octane numbers, H/C ratio, calorific values, density, vapor pressure, etc. Therefore, it is vital that the molecular composition of the surrogate is as close to that of the reference gasoline as possible, while keeping the fuels complexity relatively low, such that it can be modeled kinetically. For the

TABLE 1 A comparison of the compositions and properties of reference gasoline PR5801 and the formulated 5-C surrogate

Gasoline PR5801 component	Gasoline PR5801 (vol%)	5-C surrogate component	5-C surrogate (vol%)
Paraffins	47.1	iso-Octane	50.5
		n-Heptane	10.8
Aromatics	26	Toluene	25.9
Olefins	7.9	1-Hexene	8.1
Ethanol	4.7	Ethanol	4.7
RON	95.4		95.1
MON	86.6		87
H/C	1.93		1.9
Octane sensitivity	8.8		8.1
Antiknock index	91		91.05

purposes of surrogate development, the molecular composition of gasoline can be categorized into several molecular groups: paraffins (*n*- and iso-paraffins), naphthenes, aromatics, and olefins. It is also now common for commercially available gasolines to include oxygenated compounds, such as alcohols. For the formulation of the 5-C surrogate, iso-paraffins and *n*-paraffins are represented by iso-octane and *n*-heptane, respectively. These molecules are well characterized in terms of their autoignition properties and have been applied to a vast amount of studies as surrogate fuels, either in the form of PRF, which include iso-octane and *n*-heptane exclusively,[19,20,55,56] or more complex fuel mixtures.[36,39,57] The aromatic component of the gasoline is emulated by toluene, which is also well characterized, leading to commonly used three-component surrogate mixtures, often titled TRF.[28,29] Olefins are represented here by 1-hexene. This provides a cost-effective and functional emulation of the olefin component of gasolines and has been used in previous studies to similar effect.[33,58] Lastly, alcohols are represented by the addition of ethanol to the surrogate mixture, as this is in direct correlation to the alcohol content of commercially available gasolines.

The comparative properties and compositions of the reference gasoline and the 5-C surrogate can be seen in Table 1, wherein the "octane sensitivity" refers to the difference between RON and MON values, and the "antiknock index" is the mean value of the RON and MON. It can be seen that the developed 5-C surrogate matches much of these critical properties closely, particularly values for RON and MON. However, it can also be seen that the 5-C mixture contains a much greater percentage of paraffins than the gasoline. This is due to the lack of naphthenes in the surrogate, which are present in the gasoline. Naphthenic content is replaced by paraffins to reduce the computational burden of a more complex surrogate mixture while attempting to maintain a robust emulation of the reference gasoline.

2.2 | IDT measurement

IDT measurements were produced using the University of Leeds RCM facility, the current configuration of which can be described as a pneumatically driven single-piston design, featuring hydraulic piston locking and motion damping. The RCM operates by adiabatically compressing a compositionally and thermodynamically homogeneous fuel/air mixture, to a desired end of compression temperature and pressure state, as fast as possible (ideally the compression would be completed instantaneously). To complete this, a charge is first premixed in a separate mixing chamber. In the case of the Leeds RCM, this mixing chamber is a cylinder of 1.8×10^{-3} m^3 volume, with a maximum operating pressure of 0.5 MPa and heating functionality provided by a 2-kW band heater. Liquid fuels are introduced to the mixture on a volumetric basis, using individual syringes (for each component) for liquid components and separate gas lines for oxidizer and diluents, allowing for consistent and accurate mixture production, which negates the likelihood of cross-contamination between fuel components. Each syringe is chosen such that uncertainty in volume measurements is minimized, with an uncertainty of $\pm 0.5\,\mu L$ for the smallest volumetric fuel component. To illustrate the impact of such uncertainties, the change in simulated IDTs as a result of twice the measured uncertainties in each component can be seen in the Supporting Information. This shows that the variance in the IDT due to uncertainties in mixture preparation is expected to be small (<0.5 ms due to twice the uncertainty in each component). As the liquid component is injected, the partial pressure change due to this is measured and compared to a computed partial pressure based on the precalculated component volume, providing a secondary check that the volume of the liquid fuel component is accurate, as performed in previous studies.[59] Molecular oxygen is used as the oxidizer and an assortment of diluents ($Ar/CO_2/N_2$) are used to control the mixture specific heats,

TABLE 2 Operating parameters of the University of Leeds rapid compression machine

Parameter	Value
Maximum driving pressure	20 bar
Maximum hydraulic locking pressure	50 bar
Maximum mixing chamber pressure	4 bar
Maximum end of compression pressure	30 bar
Maximum initial pressure	1.5 bar
Maximum initial temperature	100°C
Compression ratio	9–24
Compression time	≤20 ms
Piston bore	44 mm
Piston crevice volume	3 cm^3

allowing for the production of a range of end of compression conditions. Charges are left to homogenize at the predetermined initial gas temperature for 120 min minimum, after which a sample of the charge is transferred to the combustion chamber. This combustion chamber is heated by a series of six 50-W cartridge heaters inserted into a large steel end-plug, as well as five 75-W band heaters spaced equally between the piston's resting position at bottom dead center and the combustion chamber entrance. When fired, the piston completes a full compression (230 mm stroke length) in less than 20 ms. Hydraulic oil serves as a piston locking and damping mechanism. Piston position is monitored with a Keyence model LK-G82 laser and sensor pack to provide piston displacement measurements at a rate of 20 kHz. Data from this sensor pack are used in the analysis to determine when the piston arrives at top dead center.

When compared to the most previous descriptions of the University of Leeds RCM facility,[28,29] the equipment has undergone some modification. A creviced piston head was introduced to facilitate a more homogeneous temperature environment within the combustion chamber during compression, through the suppression of boundary layer swirl vortices. The aim of this change was to help maintain the charge hot adiabatic core, allowing for the probing of longer IDTs consistently. This is of particular importance for the low-temperature autoignition of alcohol fuels (such as iso-butanol), where it is necessary to eliminate the possibility of inhomogeneous ignition cases. The operating regime of the University of Leeds RCM can be described by the parameters shown in Table 2.

The adiabatic core assumption is applied in the precalculation of all RCM test conditions. This assumption allows for the prediction of the end of compression thermodynamic conditions, based on the initial gas temperature, pressure, and ratio of specific heats. Equation (1) describes this assumption.

$$\frac{T_c}{T_i} = \left(\frac{P_c}{P_i}\right)^{\frac{\gamma-1}{\gamma}}. \quad (1)$$

Here, T_i and T_c are the initial temperature and temperature at the end of compression, P_i and P_c are the initial and compressed pressures and γ is the ratio of specific heats for a given fuel/air mixture. For a fixed initial temperature, a range of end of compression conditions can be produced through the manipulation of the initial pressure and the ratio of specific heats, which in turn can be controlled through the addition of different diluents in varying amounts (as mentioned previously). Typically, monatomic gases (such as argon) allow for the investigation of higher temperatures, whereas polyatomic gases (such as carbon dioxide) allow for the probing of lower temperatures.[60]

For the purposes of this study, the derived IDT is defined as the time difference between the end of compression (as dictated by the piston displacement laser measurement) and the point of autoignition. This point of ignition is defined as the global maximum rate of pressure increase. Nonreactive pressure histories are also collected for each RCM experiment and are provided in the Supporting Information. These are produced by replacing the mixture oxygen content with nitrogen and repeating the experiment under the same temperature and pressure conditions. The similar thermophysical properties of oxygen and nitrogen allow for the assumption of consistent heat loss behavior between the nonreactive and reactive cases. Pressure data provided from these nonreactive tests are used to produce a real volume history of the RCM, which can in turn be used to produce variable volume simulations. This method is beneficial in that it allows for simulations to account for heat losses which occur during the operation of the RCM, an issue that is exacerbated by long IDTs. Nonreactive pressure data (alongside reactive pressure data) is also used in the calculation of RCM heat release rates (HRRs). RCM pressure histories are collected using a Kistler 6045A dynamic pressure transducer, at a frequency of 100 kHz, which is sufficient to resolve low-temperature heat release (LTHR) and intermediate temperature heat release (ITHR) behavior. However, to resolve rapid high-temperature heat release (HTHR) behavior a higher capture frequency (~1 MHz) would be required. As such, HTHR behavior as deduced by HRA is rarely discussed in the article. To show the high degree of repeatability for the RCM and HRA applied in this study, figures can be found in Supporting Information which show HRA for several individual RCM "shots." The relationship between the derived LTHR and first-stage ignition is also shown in the Supporting Information , displaying that the two events coincide, as would be expected.

RCM experiments were performed for the "neat" fuels (reference gasoline PR5801, its 5-C surrogate and

TABLE 3 A list of fuel blends investigated in the University of Leeds RCM and the associated end of compression temperatures tested. All experiments presented in this study occur at a precalculated compressed pressure of 20 bar, under stoichiometric conditions

Blend	Temperatures (K)
Gasoline (PR5801)	675–870
Gasoline iB05	710–870
Gasoline iB10	
Gasoline iB20	
Gasoline iB30	
Gasoline iB50	
Gasoline iB70	
5-C Surrogate	675–870
5-C iB05	710–870
5-C iB10	
5-C iB20	
5-C iB30	
5-C iB50	
5-C iB70	
iso-Butanol	

iso-butanol), as well as blends of 5–70% iso-butanol by volume with both the reference gasoline and the 5-C surrogate. Experiments were performed at stoichiometric conditions, a compressed pressure of 20 bar and end of compression temperatures of 675–870 K for the reference gasoline and 5-C surrogate and 710–870 K for all blends. A catalog of test cases is described in Table 3.

2.3 | HRR analysis

Goldsborough et al.[54] have shown in previous work that HRA can be applied effectively to RCM experiments, facilitating the investigation of low-temperature heat release behavior for a wide range of thermodynamic conditions. This study applies similar methods for the calculation of HRRs from experimental RCM reactive pressure histories. Initially, the energy conservation equation (Equation 2) is applied to the gas in the RCM reaction chamber:

$$\frac{dU_s}{dt} = \dot{Q}_{\text{chem}} - \dot{Q}_{\text{wall}} - \dot{W}_{\text{piston}} - \dot{H}_{\text{out}} + \dot{H}_{\text{in}}, \quad (2)$$

where U_s is the total sensible internal energy, $\dot{Q}_{\text{chem}}$ is the rate of heat released, $\dot{Q}_{\text{wall}}$ is the rate of heat exchange with the chamber walls, $\dot{W}_{\text{piston}}$ is the rate of work done by the piston on the gas, and $\dot{H}_{\text{out}}$ and $\dot{H}_{\text{in}}$ are the rates of enthalpy flow out and in of the reaction chamber, respectively. As previously described, the adiabatic core assumption is applied to define the simplified RCM system, such that it is composed of a single volume consisting of both burnt and unburnt gases. In this simple system, any reactivity that may be present in the cool boundary layer is neglected. It is assumed that the contents of the combustion chamber are fully homogeneous in terms of pressure and that the contents behave as an ideal gas. Nonreactive RCM tests provide pressure (and volume) histories, which are applied to empirically account for heat losses from the RCM system over the course of a test. By applying Equation (2) under these conditions, and assuming that the piston trajectory is identical between both reactive and nonreactive cases, it can be shown that[54]

$$\text{HRR} = \frac{\gamma}{\gamma - 1}\frac{dV}{dt}(P - P_{\text{nr}}) + \frac{1}{\gamma - 1}V\left(\frac{dP}{dt} - \frac{dP}{dt}|_{\text{nr}}\right) - \frac{PV}{(\gamma - 1)^2}\left(\frac{d\gamma}{dt} - \frac{d\gamma}{dt}|_{\text{nr}}\right), \quad (3)$$

where γ is the ratio of specific heats, V is the reaction chamber volume (as calculated from the nonreactive pressure history for the given experiment case), P is the pressure in the chamber and the suffix "nr" denotes properties of the nonreactive case. From this equation, it is possible to calculate the HRR at any time step, given the appropriate reactive and nonreactive pressure histories.

The Cantera[61] python library and a combined iso-butanol/gasoline surrogates mechanism (detailed in Section 2.4) are applied to each RCM experiment case to calculate the temperature-dependent specific heats at each time step, as required to solve Equation (3). Specific heats for each species are determined using NASA 7-coefficient polynomial parameterization, as dictated by mechanism thermodynamic data. This allows the model to account for the changing gas properties during the experiments. Pressure traces are aligned for this model at the end of compression, as determined by the RCM piston displacement measurements, such that the end of compression is equivalent to piston top dead center. The accumulated heat release (aHR) is calculated as the time-integrated HRR. All HRRs and aHRs presented in this study are normalized by the lower heating value of the fuel mixture for each blend, allowing for comparisons between blends of their proportional heat release behavior.

2.4 | Model simulations and sensitivity analysis

Kinetic modeling of the IDTs is performed using the CHEMKIN-PRO[62] software, wherein the RCM system is simulated by a single zone, zero-dimensional homogeneous reactor. Constant volume and variable volume simulations are performed as part of this study. Case-dependent

volume histories are applied to produce variable volume IDT simulations, which account for some of the non-ideal characteristics of RCM operation, including heat losses and radical buildup during the compression phase. Volume histories are calculated from nonreactive RCM experiment pressure traces (as is standard practice).[63,64] The time-dependent volume is calculated from the pressure at a given time using the temperature-dependent specific heat for the case fuel/air mixture and isentropic core relationships.[6] A combined mechanism based on that of Sarathy et al. which includes all butanol isomers,[1] and the Lawrence Livermore National Laboratories (LLNL) "Gasoline Surrogate" mechanism[33] is applied to produce modeling results. It is understood that some improvements have been made to the LLNL "Gasoline Surrogate" mechanism; however, this updated mechanism has not been made widely available.[65,66] Thus, this study applies the most up to date widely available version of the LLNL "Gasoline Surrogate" mechanism. Based on the work of Agbro et al.,[29] the mechanism was updated such that the rate constant for the reaction $C_6H_5OH + CH_3 \Leftrightarrow C_6H_5CH_3 + OH$ was consistent with that provided by Seta et al.,[67] which is the source for much of the toluene oxidation chemistry present in the mechanism. The full combined mechanism consists of 8396 (6524 reversible) reactions and 1983 species. Much of the thermodynamic data in this mechanism is predicted with the use of Benson's GA values, as documented in the mechanism sources. Using mechanism reduction tools, unaccessed species and reactions (such as those required for the oxidation of the other butanol isomers) were eliminated from the mechanism. This was performed using the Reaction Workbench software,[68] applying the direct relation graph with error propagation reduction method.[69] This simple elimination of irrelevant species and reactions produced a mechanism of 4322 reactions (3643 reversible and 2403 reactions with defined reverse rate parameters) and 872 species. This mechanism is provided in the Supporting Information in both CHEMKIN and Cantera formats. The IDT in these cases is defined as the time difference from the end of compression to the maximum peak in OH concentration, which often serves as an analogue for the point of ignition in models of this kind.

To investigate discrepancies between experimental IDTs and simulated results, as well as to highlight important reactions and the driving thermochemical behavior, a sensitivity analysis was conducted at several modeled conditions. A local A-factor sensitivity analysis was performed using the CHEMKIN-PRO[62] software to determine the sensitivity and potential influence of each reaction on the peak concentration of OH. The radical OH is selected as the target for this analysis as it is known to serve as the main chain carrier for hydrocarbon autoignition and oxidation, with a rate of production which is closely linked to the overall reaction rate.[70,71] CHEMKIN-PRO[62] utilizes a modified version of DASPK[94] which applies backward differentiation formula methods to solve the system of ordinary differential equations (ODEs) and produce the desired sensitivity coefficients.[72,73] Furthermore, a brute force sensitivity analysis was performed to assess the impact of uncertainties in the thermodynamic properties of each species (namely the enthalpy of formation) on the overall IDT. To achieve this, the NASA polynomial[74] a_6 was modified, ensuring that only the enthalpy of formation for the species was affected, without influencing the species entropy or specific heat. The standard enthalpy of formation was modified individually and independently for each species by a constant value of +5 kJ mol^{-1}, which is well within the uncertainty bounds proposed for many oxygenated fuel radical species[75] but large enough to facilitate the identification of significantly important species. Such perturbations will only identify species which take part in reversible reactions, wherein the reverse rate parameters are not specified. Hence a combined approach which explores both reaction rate and thermodynamic data is utilized in this study. The sensitivity coefficient corresponding to this change can be calculated via $SC = (\tau_{mod} - \tau_i)/\tau_i$, where SC is the sensitivity coefficient for a given species, τ_{mod} is the IDT after the enthalpy modification for this species and τ_i is the initial (unmodified) IDT for this condition. Diluent species and molecular oxygen are excluded from thermodynamic sensitivity analysis. The high sensitivity of molecular oxygen is known, due to its presence in many important reactions such as initiation oxygen additions, and the molecule's thermodynamic data are assumed to be known with absolute certainty.[52] Therefore, this value is discounted to prevent the dilution of further normalized sensitivity values. In addition, while we acknowledge that in reality correlations exist between enthalpy values for different species, they have been neglected here as they are only known for smaller species present within Active Thermochemical Tables (ATcT).[76,77] Such information is not known for the larger fuel-related species within the mechanism and therefore it is not possible to account for such correlations. The aim of this work is to identify important species that are key to the observed ignition behavior, rather than attempting to assess the overall uncertainty in the chosen targets, which would necessitate taking correlations into account. As part of the analysis, heats of formation for the key-identified species from the mechanism are compared with values available in Burcat's latest thermochemical tables, based on experimental, ab initio calculation, and more recently ATcT methods.[75] Values for both local OH and brute force enthalpy sensitivity analysis are normalized by the largest corresponding values to produce lists of normalized sensitivity coefficients.

INTERNATIONAL JOURNAL OF CHEMICAL KINETICS WILEY

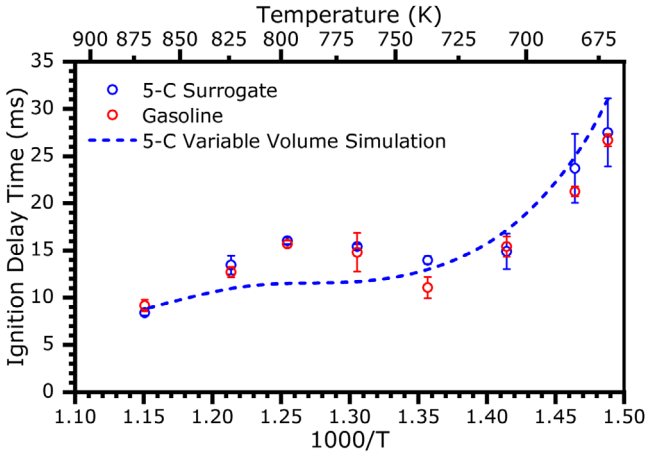

FIGURE 1 Surrogate representation of the reference gasoline IDT profile, including variable volume simulation predictions. Symbols represent experimental data. Dashed line shows model predictions. Error bars represent 2σ. All results are recorded at $P_C = 20$ bar, $\Phi = 1$ [Color figure can be viewed at wileyonlinelibrary.com]

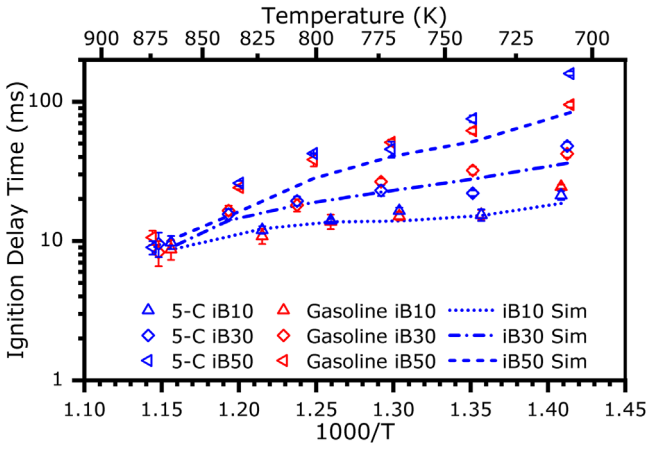

FIGURE 2 Surrogate representation of the reference gasoline IDT profile at blends of 10, 30, and 50% iso-butanol by volume, including variable volume simulation predictions. Symbols represent experimental data. Dashed lines show model predictions. Error bars represent 2σ. All results are recorded at $P_C = 20$ bar, $\Phi = 1$ [Color figure can be viewed at wileyonlinelibrary.com]

3 | RESULTS

3.1 | Surrogate performance

Figure 1 shows the experimentally derived IDTs of the reference gasoline, its 5-C surrogate, and the variable volume simulated IDTs for 5-C. IDTs are presented as the mean of four to six individual experiments, with error bars representing twice the standard deviation of each case. Experimentally, the 5-C surrogate provides an excellent representation of the reference gasoline. The general IDT profiles appear very similar for the two fuels, including similar values at the low and high temperatures, as well as within the NTC region. An exception to this relationship can be found at 740 K. At this condition, the 5-C surrogate shows a significantly longer IDT (~3 ms longer) than the reference gasoline leading to the appearance of a less intense NTC region. This behavior is somewhat predicted by the 5-C variable volume simulation, which shows an NTC region much shallower than that of the reference gasoline. However, under these conditions, the NTC behavior predicted by the variable volume simulation substantially overpredicts the reactivity displayed by the 5-C surrogate. In contrast, at the lower end of the temperature regime, the model slightly overpredicts the IDT of the 5-C surrogate. These differences indicate that the combined mechanism applied does not accurately reproduce the ignition behavior of one or multiple of the 5-C surrogate components. This misrepresentation is investigated further in this study, through the application of sensitivity analysis techniques since it is likely to be due to uncertainties in reaction rate parameters, and species thermodynamic data for fuel component related species that have been calculated through GA. It should also be noted that, in general, the 5-C surrogate displays a larger uncertainty in IDT measurements, than the reference gasoline. This is to be expected due to the added complexity of the preparation of the 5-C mixture, which requires the injection and mixing of five individual liquid components.

Figure 2 shows the experimentally derived IDTs for the blended conditions iB10, iB30, and iB50, for the 5-C surrogate and reference gasoline, as well as variable volume simulation results for these 5-C and iso-butanol blends. It can be seen in this figure that the 5-C surrogate continues to provide a reasonable analogue for the reference gasoline under blended conditions, providing a good representation of the trends on blending to higher levels of iso-butanol. As expected, based on the ONs of the fuels, increasing the volume percentage of iso-butanol leads to longer IDTs, particularly at lower temperatures. However, at 710 K, the 5-C iB10 IDT is significantly shorter than that observed in gasoline iB10, and at high and low temperatures there are notable differences between the IDTs for iB50 blends. There is also a significant difference between iB30 IDTs for the two fuels at 740 K, and generally shorter IDTs for the 5-C iB30 than the gasoline blend. In general, variable volume simulations continue to underpredict the NTC intensity for each blend, which is consistent with an overprediction of reactivity for the unblended surrogate. This general failure of the model becomes more pronounced with increasing percentage of iso-butanol in the blend.

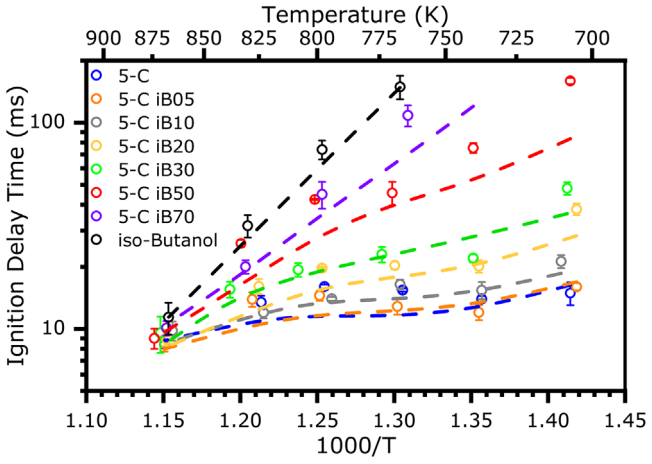

FIGURE 3 Comparison of experimentally derived IDTs for all investigated surrogate and iso-butanol blends. Symbols show experimental data. Dashed lines show variable volume simulation results. Error bars represent 2σ. All results are recorded at $P_C = 20$ bar, $\Phi = 1$ [Color figure can be viewed at wileyonlinelibrary.com]

3.2 | Blending behavior

The influence of increasing iso-butanol volume percentage on the IDTs of blends can be seen in Figure 3, which shows IDT profiles for all blending ratios for the 5-C surrogate and iso-butanol fuels ($P_C = 20$ bar, $\Phi = 1$). Normalized IDTs, plotted as a function of iso-butanol content, are also available in Supporting Information, to aid the reader in identifying blending behaviors. Unlike the 5-C surrogate and reference gasoline, the IDTs of iso-butanol exhibit no NTC behavior. Instead, an Arrhenius behavior is observed, where the IDTs increase exponentially with decreasing temperature. This behavior is consistent with literature examples of iso-butanol IDTs.[6] At temperatures below 770 K, IDTs for iso-butanol could not feasibly be recorded due to the excessively long delay times. At conditions with long times between the end of compression and ignition, the adiabatic core assumption breaks down, even with the use of a creviced piston head. This breakdown leads to a higher likelihood of inhomogeneous ignition events (such as preignition) and drastically increased degrees of heat loss, which cause unreliable IDT measurements, with a low degree of repeatability.[63,78] Figure 3 shows that variable volume simulations provide a good prediction of the iso-butanol ignition delay behavior, accurately capturing the Arrhenius behavior and providing a relatively good estimate of real IDTs across the studied temperature range.

In general, at temperatures of and below 770 K, the influence of iso-butanol blending on the IDTs appears to be monotonic: increasing iso-butanol volume fraction leads to a longer IDT. The exception to this generality can be seen for the iB05 blend, wherein IDTs at temperatures of 740–800 K are shorter than those observed for the 5-C surrogate. At higher temperatures (>800 K), the IDTs for iB05 are practically the same as those for the 5-C surrogate (within reasonable uncertainty). However, there is an apparent crossover in autoignition susceptibility between the iB05 and iB10 blends at these temperatures, where the higher degree of iso-butanol blending produces shorter IDTs. At these conditions (800, 830 K), the iB10 blend also displays shorter IDTs than the original 5-C surrogate. This same nonmonotonic blending behavior can be observed in the blending of iso-butanol with gasoline, as shown in Figure 4, wherein the gasoline iB10 blends become the most reactive at temperatures of 800 K and higher. At these low iso-butanol blends, this nonlinear blending behavior may be due to the suppression of the typical NTC behavior by small amounts of alcohol. While this suppression of the NTC by iso-butanol is also present in the larger iso-butanol content (e.g., iB50, iB70) conditions, the influence of the larger amounts of iso-butanol is such that the IDTs have increased drastically beyond those of the 5-C surrogate and gasoline, suppressing the overall reactivity of the fuel. Similar behavior has been observed in the blending of *n*-butanol with gasoline,[28,29] where suppression of the fuels NTC region by *n*-butanol was observed to produce an IDT crossover at 20% *n*-butanol. Given the longer ignition times and Arrhenius profile of iso-butanol when compared to *n*-butanol,[6] it is not unreasonable to speculate that this crossover would appear at blends of lower iso-butanol volume.

As the blends iso-butanol volume fraction is increased to 20%, 30%, and 50%, IDTs increase across the temperature regime. The NTC behavior observed for the 5-C surrogate and gasoline slowly shallows out, with only a mild indicator of this behavior at the iB50 blend conditions. Also, perhaps due to this shallowing of the NTC, IDTs for iB20 and iB30 conditions (apart from the lowest temperature condition) are very similar, particularly in the NTC region. This impacts on the choice of blends that would be most appropriate for use in a SI engine based on these data, as the marginal knock resistance gains must be balanced against any changes in the overall calorific value of the fuel blend, due to the addition of 10% more iso-butanol by volume. The iB50 blend shows a drastic increase in IDTs from the iB30 blend, with IDTs at higher temperatures very similar to those seen in the pure iso-butanol fuel. However, the iB70 blend produces IDTs shorter than those of the iB50 blend at these same temperatures. This blend displays the Arrhenius IDT behavior characteristic of the iso-butanol fuel, with no distinguishable NTC region. Again, this same nonmonotonic behavior is witnessed for gasoline blends as well as 5-C blends (Figure 4). Like iso-butanol, IDTs at the lowest temperatures could not be captured due to the

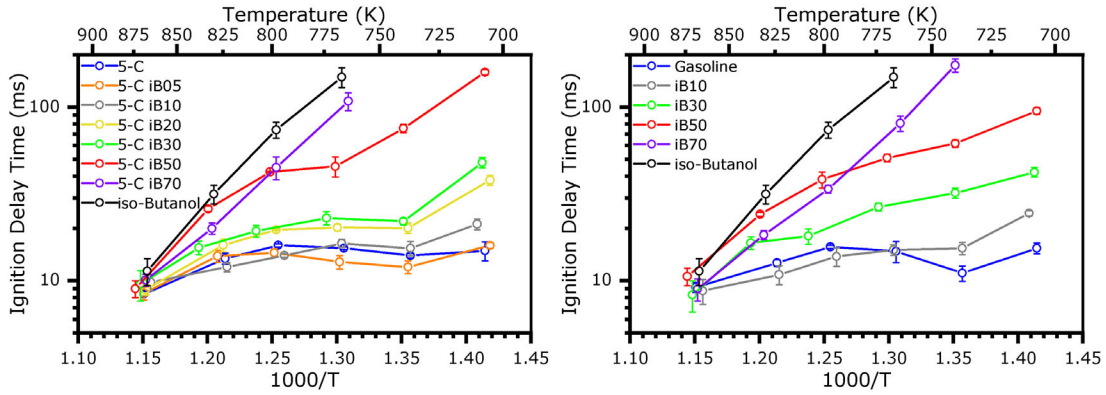

FIGURE 4 Experimentally derived IDTs for the investigated 5-C (left image) and gasoline (right image) blends with iso-butanol. Symbols show experimental data. Solid lines connecting each point are displayed for clarity. $P_C = 20$ bar, $\Phi = 1$ [Color figure can be viewed at wileyonlinelibrary.com]

exceedingly long delays and associated heat loss effects. In the midtemperature range, iB70 does produce longer IDTs than iB50, but due to the mild NTC present in the iB50 fuel the two IDT profiles crossover, leading to the aforementioned shorter iB70 IDTs. This provides a further example of the effects of NTC suppression by the iso-butanol fuel component.

While variable volume simulations correctly predict the ignition delay behavior at the lowest investigated temperatures (increasing iso-butanol volume at these conditions increases IDT), they fail to predict several other features of these blends. The failure of the mechanism to predict the 5-C NTC region has been mentioned previously, and this is a common feature for all the lower iso-butanol blends (iB05, iB10, iB20). Similarly, to the 5-C surrogate, variable volume simulations also show a slight underprediction of reactivity at the lowest temperatures for the iB05 blend. However, as the iso-butanol volume percentage increases beyond 5%, simulations begin to overpredict reactivity at these same temperature conditions, with an increasing degree respective to the iso-butanol volume percentage of the blend. At iB50, simulations overpredict reactivity throughout the regime and provide little indication of any NTC. While it seems logical to attribute some of this difference to experimental heat losses at longer IDTs, it should be noted that not only should variable volume simulations provide a sufficient account of this but also pure iso-butanol does not show such a disparity. This may indicate that the gasoline surrogate's aspect of the mechanism[33] is the source of simulation issues, which is further supported by the mechanism's inability to reproduce the NTC region.

3.3 | Heat release analysis

To further investigate the nonlinear blending behavior observed and provide targets for further model investigation, HRRs are extracted and analyzed from the RCM experiments. Figures 5 and 6 show the experimental and simulated HRRs prior to the main ignition event plotted against the aHR and time from the maximum pressure gradient, respectively, at temperatures of 710, 770, and 830 K. LTHR is common in degenerately branched systems and describes exothermic events that occur before the main stage of heat release, which describes the autoignition event.[79] LTHR is indicated by a relatively sharp peak in HRR and an associated rise in pressure, which also produces a visible CH_2O^* chemiluminescence and is considered to be chemically due to the decomposition of ketohydroperoxides to produce multiple OH radicals.[54] In some cases, LTHR may be followed by an intermediate stage of heat release (ITHR), which also occurs before the autoignition event. ITHR is less well understood but can be described as a gradual rise in HRR (and therefore pressure), due to coupled self-heating processes. The driving chemistry of ITHR is less well understood than LTHR, but it is thought to be due to RO_2 direct elimination reactions, producing an alkene/carbonyl/ether species + HO_2, followed by the recombination reactions of HO_2. This leads to an accumulation of large amounts of H_2O_2, which, as temperature slowly increases, will ultimately decompose into OH radicals, causing the main stage of heat release and autoignition.[80]

At 710 K, the experimentally derived data in Figure 5 shows a clear single LTHR peak for the 5-C surrogate. The model, however, predicts two stages of LTHR, with the second stage appearing as a small peak, shouldering an initial larger peak. Also, the experimentally derived peak is somewhat lower in magnitude than the model peak and both the LTHR initiation and the peak LTHR occur earlier than predicted by the model. The addition of small amounts of iso-butanol produces a clear impact on the LTHR behavior of the fuels, reducing the peak HRR in the LTHR region and flattening the LTHR

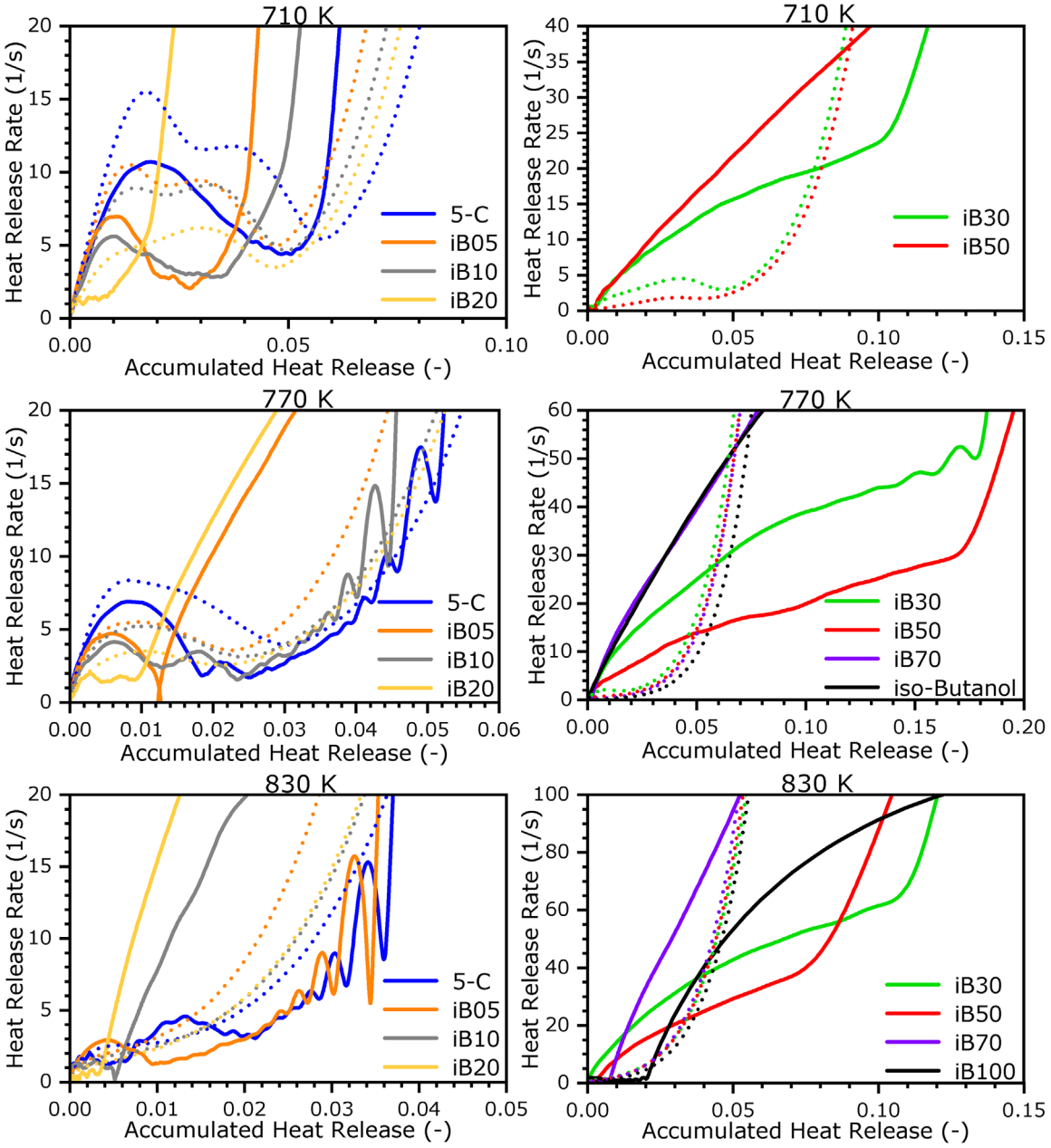

FIGURE 5 The relationship between LTHR and aHR for surrogate and iso-butanol blends. Solid lines show results calculated from RCM pressure histories. Dashed lines show results calculated from kinetic simulations. All results are recorded at $P_C = 20$ bar, $\Phi = 1$ [Color figure can be viewed at wileyonlinelibrary.com]

profile. Even for iB05 experimental results, there is a clear LTHR peak reduction and the appearance of a mild shoulder to the LTHR peak, indicating a second, much smaller phase of LTHR. When compared to the experimental 5-C surrogate results, the HRR profile is extended, with LTHR beginning earlier and continuing longer, but at lower magnitudes. This is also true for iB10, which further reduces the peak LTHR value at an earlier time and displays a flatter, more constant HRR profile. These lower peak LTHR values coincide with an increase in IDTs between blends. As in the 5-C surrogate simulations, iB05 and iB10 peak LTHR is overpredicted by the model and begins later than the calculated heat release. The simulations display two distinct LTHR humps, which are clearly not present in the experimentally derived data, with much higher peak heat release than that calculated from experimental pressure traces. In terms of aHR, simulations predict that ignition occurs at a slightly higher aHR for 5-C than iB05 and iB10, which coincides with an increased rate of HRR for the surrogate. From observing higher iso-butanol blends, it appears that accumulating more heat release prior to ignition indicates shorter IDTs, which is intuitive as this would

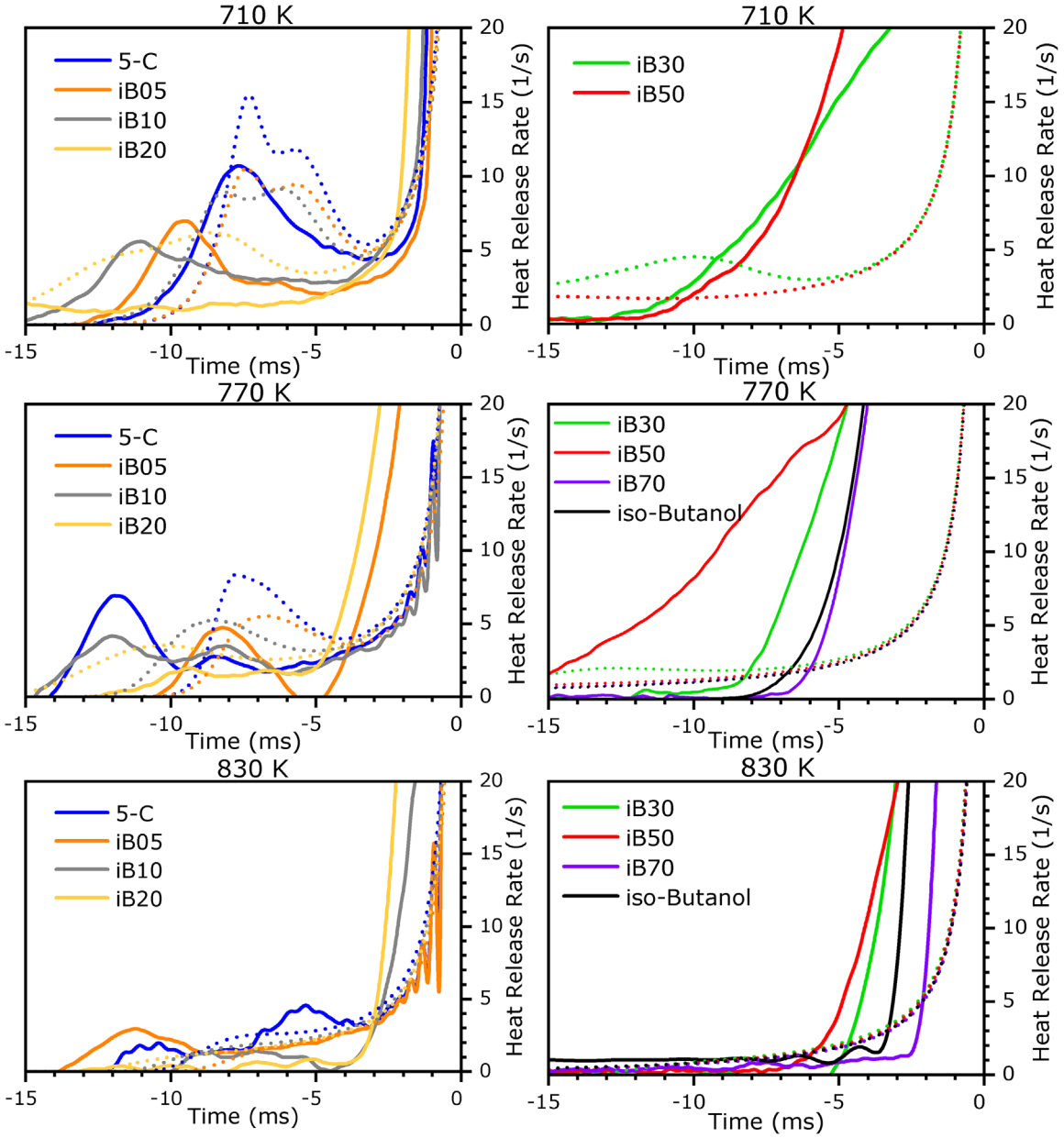

FIGURE 6 The relationship between LTHR and time from maximum heat release, for surrogate and iso-butanol blends. Solid lines show results calculated from RCM pressure histories. Dashed lines show results calculated from kinetic simulations. All results are recorded at $P_C = 20$ bar, $\Phi = 1$ [Color figure can be viewed at wileyonlinelibrary.com]

also indicate elevated temperature and pressure conditions. Main stage ignition also occurs at much smaller values of aHR in experiments than the simulations predict. At blends of higher iso-butanol volume percentage, LTHR is completely absent at 710 K in the experimental data, despite the prediction of small amounts of LTHR by the model. The model prediction also shifts at these higher blending ratios, from predicting a two-stage LTHR dominated by the first stage, to being dominated by the second stage before almost entirely disappearing. A region of ITHR can be observed in the HRR analysis of iB30 and iB50, leading into the main phase HRR. Initially, it was thought that this may represent inhomogeneous ignition events, such as preignition heat release (PIHR). However, previous examples of PIHR observed in the University of Leeds RCM have displayed a characteristically large degree of variance between individual RCM "shots," whereas the behavior observed in these cases for iB30 and iB50 is highly repeatable. Significant efforts have recently been made to modify the University of Leeds RCM to identify and remove undesirable PIHR behavior, eliminating the previously prevalent phenomenon during the measurement of iso-butanol IDTs. The mild ignition behavior observed for these blends may be due to the influence of iso-butanol on

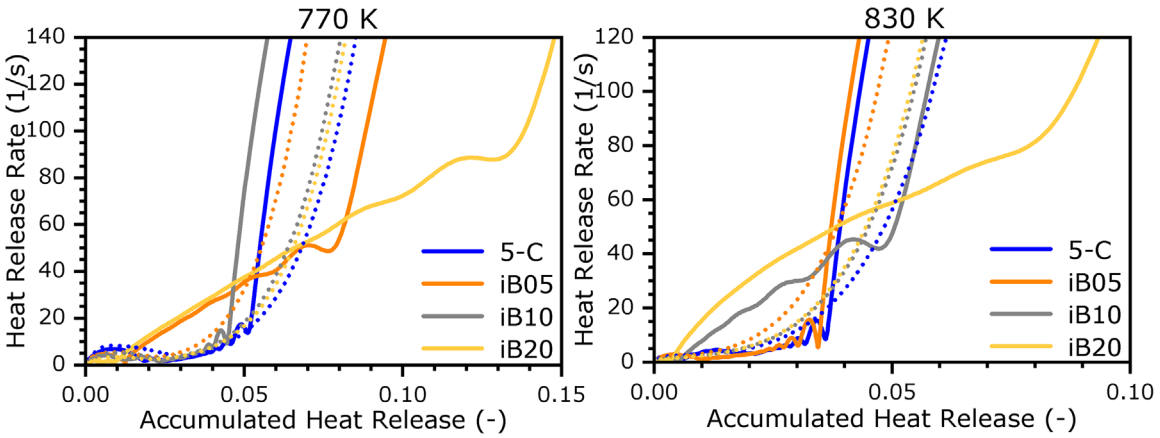

FIGURE 7 Demonstrations of intermediate heat release phenomena. Solid lines show results calculated from RCM pressure histories. Dashed lines show results calculated from kinetic simulations $P_C = 20$ bar, $\Phi = 1$ [Color figure can be viewed at wileyonlinelibrary.com]

the radical pool during autoignition, and the resultant suppression of LTHR due to the role of iso-butanol as a radical scavenger. Historically, experimental measurements have proposed a spatially homogenizing effect of LTHR on temperature nonuniformities generated during piston motion and gas compression.[81] Suppression of this behavior may allow for the development of repeatable mild ignition behavior, if the underlying causes for spatial inhomogeneities in the combustion chamber are repeatable.

At 770 K (within the NTC region for many of the investigated fuels) both the 5-C surrogate and iB10 display two distinct stages of LTHR, unlike the lower temperature of 710 K. For the 5-C surrogate, the first LTHR peak is the most prominent, whereas both peaks show equal prominence in iB10. This behavior is not predicted by the model, which produces only one stage of LTHR. However, iB05 does only show one LTHR peak, consistent with simulations. At this condition, iB05 also produces shorter IDTs than both the iB10 and 5-C surrogate (a behavior not predicted by simulations). This would appear to indicate that the delayed release of total LTHR due to two distinct stages of initial exothermicity, as opposed to a single stage, reduces the autoignitive propensity of the fuel, increasing IDTs. This is further validated by comparison with simulated results, which display large underpredictions of IDT for the 5-C surrogate and iB10 at this condition, while also predicting a single stage of rapid heat release. On the other hand, the prediction of iB05 IDT is relatively good, as is the prediction of the LTHR profile. For all these results, however, once again simulations overpredict the magnitude of the LTHR peak and underpredict the time (from the maximum HRR) at which this peak occurs. The unusual behavior of iB05 (when compared to its neighboring blends) can be further identified in the relation of HRR and aHR. While the 5-C surrogate and iB05 show distinct phases of LTHR leading into a sharp main phase HRR, this transition is somewhat muted for iB05, which does not show such a sharp rise in heat release. Instead, iB05 appears to show a phase of ITHR (as shown in Figure 7), as well as LTHR. This ITHR shows a much shallower gradient than that seen in the main phase heat release but will lead to more highly elevated temperature and pressure conditions than if the ITHR did not occur, causing the main phase heat release to occur earlier. Calculated results for iB20 show some small LTHR at this condition, which is predicted by simulations but largely overpredicted in terms of intensity. This then transitions into a gradual ITHR region. Ignition for iB20 occurs at a much larger aHR than for iB05 because of the fuel's higher autoignitive resistance, due to the higher proportion of the less reactive iso-butanol. Blends of 30% and 70% iso-butanol show no LTHR but do show ITHR of progressively lower intensity, whereas iB70 and iso-butanol (which show the longest IDTs at this condition) only show a main stage heat release of relatively low HRR. This would appear to indicate that, as predicted, the addition of iso-butanol suppresses the typical alkane chemistry, entirely removing the characteristic LTHR behavior at blends of 30% iso-butanol and above at this condition. Instead, the behavior transitions to an ITHR behavior, which is not characteristic of either pure iso-butanol or the 5-C surrogate.

Again, at 830 K the 5-C surrogate experiments show two distinct phases of LTHR, whereas simulations predict only one small phase of LTHR. This, as was the case for the 770 K condition, coincides with a significant overprediction of reactivity by the model, further indicating that the lack of two-stage LTHR representation at these temperatures is a cause of the simulations inability to reasonably predict the NTC IDT behavior. Similarly, the simulations fail to reproduce the LTHR behavior of iB05. The blend shows an early LTHR peak in experiments, but simulations predict some small LTHR just prior to ignition.

This coincides with a large overprediction of iB05 reactivity, as has been a common feature within the NTC region. For iB10, the simulation and experimental results produce a similar LTHR profile, with the heat release occurring at roughly the same time. As would be consistent with observations for other blends, this coincides with a correct prediction of the IDT by the simulation. Furthermore, at this condition the IDTs of iB10 have crossed over with the 5-C surrogate and iB05, producing the lowest IDTs out of all the blends at 830 K. Upon investigation of the aHR, similar behavior can be observed as was seen for iB05 at 770 K: a phase of ITHR follows the LTHR, elevating temperature and pressure conditions within the reactor, which is not present in the other lower iso-butanol content blends (shown in Figure 7). For higher blends, the behavior is similar as reported for 770 K. At 830 K however, IDT results show a crossover between iB50 and iB70 blends, wherein iB50 IDTs become longer than the higher blending ratio. This does not coincide with any change in LTHR behavior for iB70, which still produces no distinguishable LTHR or ITHR, and does not undergo any NTC behavior as iB50 does.

There is little real-world experimental data from fundamental experiments (such as from RCMs) available, which could help to quantify preliminary exothermicity events such as LTHR and ITHR. Heat release analyses such as those produced in this study and others[54,82,83] provide an opportunity for this and for the improvement of kinetic models by serving as an additional validation target. The current work shows that the chosen model fails to reproduce the experimentally derived heat release profiles to lesser or greater extents in different temperature regions, and that this failure may underlie further global model failures, such as the overprediction of reactivity.

3.4 | Sensitivity analyses

Potential kinetic and thermodynamic reasons that may underlie the inability of the model to accurately predict IDTs for the investigated fuels are further investigated here through the application of sensitivity analyses of both reaction rate and thermodynamic model input parameters. Figures 8–10 show the normalized OH sensitivity analysis results for the three temperature conditions: 710, 770, and 830 K, for the 5-C surrogate, iB30, and iso-butanol, respectively. Here a positive value indicates that an increase in the rate constant leads to an increase in the OH concentration, which serves as an analogue for reactivity. Figure 11 shows brute force normalized sensitivity analysis results for the species thermodynamic sensitivity analysis of the 5-C surrogate at temperatures of 710, 770, and 830 K. Here a positive value indicates an increase in IDT, and therefore

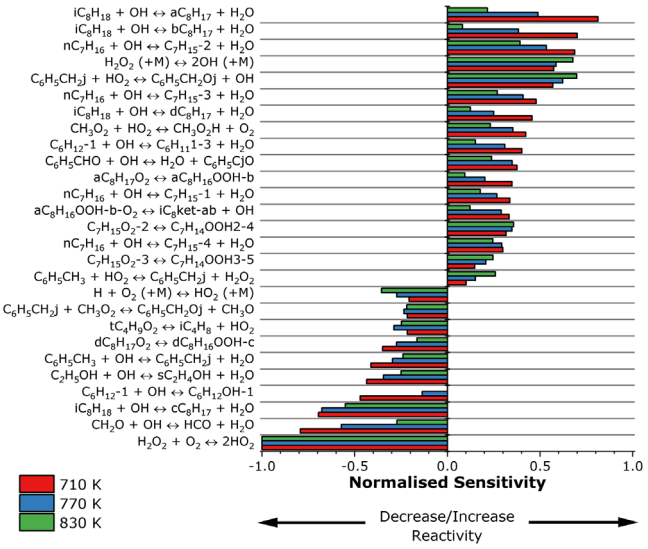

FIGURE 8 Normalized local OH sensitivity analysis results for the 5-C surrogate. $P_C = 20$ bar, $\Phi = 1$ [Color figure can be viewed at wileyonlinelibrary.com]

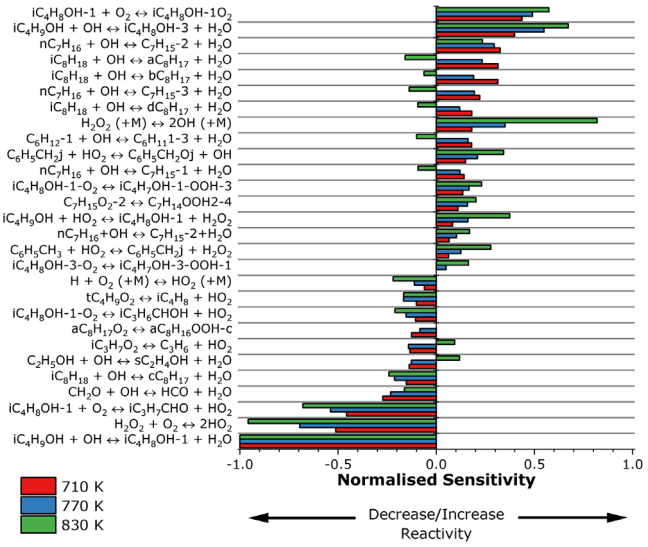

FIGURE 9 Normalized local OH sensitivity analysis results for the iB30 blend. $P_C = 20$ bar, $\Phi = 1$ [Color figure can be viewed at wileyonlinelibrary.com]

a decrease in reactivity. Each of these is limited to displaying the top 20 values (at each temperature investigated) in terms of normalized sensitivity for both local OH and thermodynamic sensitivity analyses, for the sake of brevity. A species dictionary is provided in Supporting Information, covering all the species presented in local OH and thermodynamic sensitivity analysis.

At the lowest temperature of 710 K, 5-C surrogate simulations provided a reasonable representation of measured IDTs. As can be observed in the local OH sensitivity analysis in Figure 8, reactivity at this condition is dictated

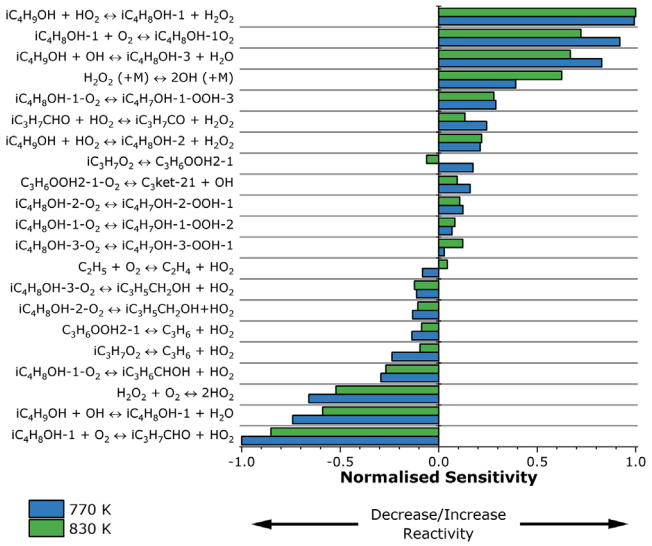

FIGURE 10 Normalized local OH sensitivity analysis results for iso-butanol fuel. $P_C = 20$ bar, $\Phi = 1$ [Color figure can be viewed at wileyonlinelibrary.com]

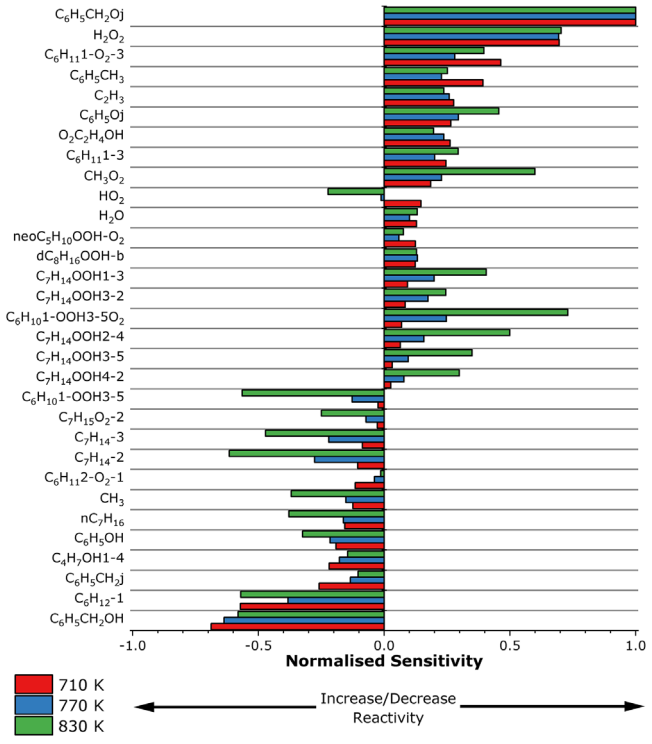

FIGURE 11 Normalized sensitivity coefficients of IDTs on enthalpy of formation, for the 5-C surrogate. $P_C = 20$ bar, $\Phi = 1$ [Color figure can be viewed at wileyonlinelibrary.com]

by typical low-temperature alkane oxidation chemistry, with hydrogen abstraction by OH from *n*-heptane and iso-octane (primarily via the primary and secondary sites) promoting reactivity. The hydrogen abstraction of ethanol and toluene by OH radicals is key to the reduction of reactivity at this temperature, due to the consumption of OH radicals, producing relatively unreactive fuel radicals and water. Also, hydrogen abstraction at the tertiary iso-octane site is highly negatively sensitive due to the lack of low-temperature chain branching pathways from the resultant radical and production of relatively unreactive olefin species.[84] Hydrogen abstraction from 1-hexene appears as a positively sensitive reaction at this relatively low temperature. This is expected as the relatively high reactivity of 1-hexene is thought to initiate low-temperature reactivity.[33] The large negative sensitivity of formaldehyde reacting with OH radicals to produce a water molecule and formyl is apparent at all temperatures for the 5-C surrogate, due to the termination of relatively highly reactive OH. The production of $2HO_2$ from the reaction of H_2O_2 and molecular oxygen is also highly negatively sensitive. The reverse of this reaction is important for the generation of the H_2O_2 pool which will ultimately decay into 2OH radicals, leading to the main ignition event.

For iB30, it can be seen that iso-butanol oxidation reactions now dominate at 710 K, with the hydrogen abstraction from iso-butanol's primary carbon site by OH radicals being the most sensitive reaction, reducing reactivity. Further hydrogen abstraction from the resultant radical's alcohol site is also highly negatively sensitive due to the production of a relatively unreactive aldehyde, as well as the generation of the less reactive HO_2 radical from the initial OH. This behavior coincides with a large over-prediction of reactivity by the model, and this pathway has been identified as a controlling aspect of high pressure, low-temperature oxidation.[6] Alternatively, the first oxygen addition to the primary fuel radical species is sensitive in the positive direction as this opens a pathway to low-temperature chain branching. Hydrogen abstraction/initiation is favored from one of the tertiary iso-butanol sites, due to an increased propensity for low-temperature chain branching from this site. However, particularly at temperatures as low as 710 K, the elevated bond dissociation energy (BDE) at the tertiary site compared to primary and secondary sites makes abstraction from this site more difficult. This behavior is a root cause of the low reactivity of iso-butanol and therefore leads to its octane boosting quality, even when compared to other butanol isomers[1]. Similar alkane reactions are seen for iB30 as with the 5-C surrogate, but their importance is reduced due to the dominance of iso-butanol reactions.

As temperature is increased to 770 K, it would be expected that sensitivity analysis of the 5-C surrogate begins to identify reactions which are typical of NTC behavior, such as the production of olefins and HO_2 radicals from RO_2 and QOOH species, and other chain propagation and termination routes.[56,85,86] However, few of these negatively sensitive reactions appear, while

simulations largely underpredict the intensity of the NTC region. Instead, reactivity is largely dominated again by the hydrogen abstraction of alkanes, with the tertiary iso-octane abstraction again displaying a highly negative sensitivity as opposed to abstractions from the alternative sites. The reaction of benzyl radicals with HO_2 to produce benzoxy and OH radicals ($C_6H_5CH_2j + HO_2 \Leftrightarrow C_6H_5CH_2Oj + OH$) appears as more positively sensitive than at 710 K. This reaction has been identified in the literature as playing a key role in the low to intermediate temperature oxidation of toluene,[33,87] which makes up a large amount of the 5-C surrogate, so its importance is not unexpected.

Sensitivity analysis for iB30 shows that hydrogen abstraction from the tertiary iso-butanol site has relatively increased, as increasing temperatures reduce the importance of the tertiary site's high BDE. As would be expected, the dissociation of H_2O_2 into two OH radicals shows an increase in sensitivity as the initial temperature increases. For the pure iso-butanol fuel, the production of H_2O_2 via hydrogen abstraction from the primary iso-butanol site by HO_2 appears highly sensitive in driving positive reactivity, much more so than for the blended fuel. This is likely due to the consumption of a relatively unreactive HO_2 radical ultimately leading to the production of two OH radicals once temperatures become high enough for the dissociation of H_2O_2. This process is key for driving the production of OH radicals at this condition, as the lower reactivity of iso-butanol fuel will struggle to develop a large pool of OH radicals, without the assistance of the alkanes present in the blend, as indicated by much larger radical pools of HO_2 and H_2O_2. These concentrations are both an order of magnitude larger than those seen for the iB30 blend, which is in turn larger than the 5-C surrogates.

Similar features can be observed for iso-butanol at 830 K; however, the previously mentioned production of H_2O_2 directly through hydrogen abstraction is now the most sensitive reaction, due to an increase in temperatures. Also, reactions indicative of low-temperature branching pathways begin to display less relative importance. The iB30 blend displays high sensitivities for the same iso-butanol reactions as the "neat" iso-butanol fuel at this temperature but is dominated by the dissociation and oxidation of H_2O_2 to form 2OH and $2HO_2$ radicals, respectively. The former of these reactions dominates the positive sensitivities as two highly reactive radicals are produced from a largely unreactive species, whereas the latter dominates the negative sensitivities at 830 K, as the HO_2 radicals formed are relatively less reactive than the OH radicals, causing an overall loss of reactivity. The oxidation of toluene increases in significance at higher temperatures also. At this condition, simulations produce a good estimate for iso-butanol and iB30 IDTs, as they did for 770 K. Meanwhile, sensitivity analysis results of the 5-C surrogate continue to show little indication of NTC behavior, contrary to the trends seen experimentally. The only indication of this is the decomposition of the RO_2 species $tC_4H_9O_2$ to produce iso-butene and a HO_2 radical. This reaction was also present in results for 770 K at a similar relative sensitivity. The reaction $C_6H_5CH_2j + HO_2 \Leftrightarrow C_6H_5CH_2Oj + OH$ is again highly positively sensitive, as is H_2O_2 decomposition. As the OH concentration for the 5-C surrogate seems highly dependent on this benzyl reaction at conditions where the model largely fails to represent experimental data, and there is little data for rates of reactions associated with toluene oxidation at these temperatures, this would appear to be a potentially large source of model uncertainty.[33,88] It should also be noted that this reaction is much less sensitive at iB30, wherein the model produces a much better representation of the IDT profile. The model sources the reaction rate for this HO_2 radical activation to OH on the recommendation of Ellis et al.[87] which provides a rate via experimental methods. However, this produces a constant, temperature independent rate of reaction within the model which is significantly different to the temperature-dependent rates proposed later in theory-based calculations.[89] The apparent high sensitivity of this reaction in the 5-C and iB30 cases, paired with this uncertainty in the rate constant may propagate significant uncertainty into model predictions. A further possible source of uncertainty in the model may be the lack of cross-reactions in the mechanism utilized. Such reactions would represent interactions between the surrogate components, as well as interactions with fuel-specific pathways within the iso-butanol mechanism. However, the work of Gorbatenko et al. found through brute force sensitivity analysis of IDTs, that the addition of cross-reactions, such as the reactions of benzyl with *n*-butanol, butanal and 1-butene, led to negligible changes in the predicted IDTs. Therefore, it was concluded that the effect of iso-butanol on the radical pool was likely to be more influential than cross-reactions, and uncertainties within the existing thermochemical data a more likely cause of the observed discrepancies between experimental results and model predictions.

Since the localized OH sensitivity analysis appears to have indicated that the failures of the model can be found in the gasoline surrogate component of the mechanism, brute force thermodynamic sensitivity analysis is focused on the surrogate modeling only. Figure 11 shows that the thermodynamic sensitivity at all investigated temperatures is largely dominated by the enthalpies of formation of toluene and 1-hexene and their associated low-temperature oxidation intermediate species. This is expected for 1-hexene and its associated species and is consistent with the understanding that the relatively high reactivity of 1-hexene, relative to iso-octane/toluene/ethanol at typical NTC temperatures

(700–800 K),[33] drives low-temperature reactivity, as observed in the local OH sensitivity of the 5-C surrogate at 710 K. The large presence of toluene oxidation chemistry is also expected at all investigated temperatures, as toluene is known to suppress low-temperature reactivity and delay both the cool flame (in two-stage ignition) and the main ignition phase.[33] Increasing the enthalpy of formation for 1-hexene reduces the energy barrier of initiation reactions, raising the overall reactivity of the fuel. While the temperature-dependent profile of the heat of formation for 1-hexene used in the LLNL mechanism employed here largely agrees with that derived from NASA polynomials in the most recent Burcat table, Burcat proposes a high uncertainty of ±8 kJ mol^{-1} for Δh_f^{298K} for this species (as calculated via G3B3 quantum chemistry calculations). Of the hexene oxidation intermediate species, high sensitivities are also shown for RO_2 and OOQOOH species. The positive sensitivities of these species are representative of a decrease in reactivity, due to a shift in the primary and secondary oxygen addition equilibria reducing the production of the species, leading to an overall decrease in low-temperature chain branching. Toluene oxidation intermediates identified in the mechanism through this sensitivity analysis often produce temperature-dependent behavior for enthalpies of formation which differs considerably from that presented by Burcat's table, which produces enthalpies of formation for these species via G3B3 quantum chemistry calculations ($C_6H_5CH_2$, C_6H_6O, $C_6H_5CH_2Oj$, and $C_6H_5CH_2OH$). It should also be noted that the latest table presents significant uncertainties for the enthalpies of these species of up to ±8 kJ mol^{-1}.[75] These analyses echo the statements presented in the HRA of experimental RCM data, further emphasizing the importance of correctly representing LTHR behavior for predicting ignition behavior. Uncertainties in highly sensitive species, which are also chemically important in the development of this low-temperature behavior, would propagate strongly into model predictions. Therefore, it is necessary that the associated thermochemical uncertainties be minimized.

Alkane oxidation intermediates (particularly for *n*-heptane) such as QOOH species display an increasing sensitivity as temperatures enter the NTC regime. For these QOOH species associated with *n*-heptane, increasing enthalpy of formation increases the required energy to overcome the potential barrier for internal isomerization of RO_2, shifting equilibrium in the direction of reactants, and increasing IDTs in the NTC region. Since the production of the mechanisms used in this study, work by Zhang et al.[90] has developed the underlying *n*-heptane mechanism to account for new reaction classes and rate rules, as well as updating thermodynamic data based on newly optimized group values.[91] These changes were deemed by the study to produce reasonably good IDT and mole fraction predictions, while maintaining parity with rate rules applied to other alkanes such as pentane and *n*-hexane.[85,92] Similar thermochemistry and kinetic updates were also produced by Atef et al.[61] for the iso-octane submechanism. Thermochemistry for the majority of presented species is calculated via Benson's GA (as stated in the mechanism source).[33] Recent work by vom Lehn et al.[53] have shown a high sensitivity in species enthalpy of formation for groups such as OO/C/H, C/C$_2$/H/OO, and C/C/H$_2$/OO, which represent the OO and OOH moieties and their adjacent groups, as seen in alkyl hydroperoxide, peroxy, and peroxy hydroperoxide radical species (typical of low-temperature chain-branching pathways). Therefore, small errors in the associated group values have the potential to cause significant changes in enthalpy and therefore IDTs for such species. While such uncertainties in the enthalpy of formation are just one of many potential sources for error in the predictions of complex kinetic models, they are often overlooked and may have a profound impact on global model predictions. This impact is demonstrated in the Supporting Information, wherein the enthalpies of RO_2, QOOH, O_2QOOH, and alkene species associated with the low-temperature oxidation of *n*-heptane and 1-hexene have been manipulated within their uncertainty limits to produce a tuned IDT profile which demonstrates a deeper NTC as seen in the experimental data. This is simply an example of the influence of such properties on global predictions and not a recommendation for model improvement. To avoid these characteristic uncertainties of the GA method, where possible, species thermochemical properties should be determined through experimental and quantum chemical calculation methods, as has occurred to facilitate the characterization of small molecules.[46,47,93] However, where this is not feasible (due to the complexity of longer fuel radical species and oxidation intermediates), future work should be motivated towards the reduction of group uncertainties to improve the accuracy of the GA method.

4 | CONCLUSIONS

The blending of iso-butanol with a 5-C gasoline surrogate produced interesting nonlinear responses in terms of measured IDTs at low iso-butanol concentrations, similar to those previously observed for *n*-butanol blending.[28] Both iB05 and iB10 blends produced the shortest IDTs out of all blends (including the original surrogate) at low and high temperatures, respectively, displaying crossover behavior with each other and with the 5-C surrogate. These regimes of high reactivity coincide with the presence of significant ITHR after the initial LTHR, which was determined to not

be due to inhomogeneous ignition due to the high degree of repeatability displayed. As the iso-butanol concentration of the blends was increased beyond 10% by volume, the blending behavior was mostly monotonic with the exception of the highest blend investigated: iB70. This blend produced shorter IDTs than the 50% blend at high temperatures, likely due to the intense NTC suppression caused by the large concentration of iso-butanol. Local OH sensitivity analysis results indicated that on addition of increasing amounts of iso-butanol, blends become highly sensitive to iso-butanol initiation reactions through hydrogen abstraction (even at the low blending ratios), as well as the associated low-temperature oxidation pathways. This contrasts with the dominance of alkane, aromatic and olefin oxidation observed for the 5-C surrogate. Competition between hydrogen abstraction from the primary and tertiary iso-butanol sites displays a high degree of importance in common with *n*-butanol.[29] Of the four possible abstraction sites of iso-butanol, the tertiary carbon site has the highest propensity for low-temperature chain branching, but also the highest BDE of the carbon sites (the alcohol site however has a higher BDE). Therefore, it is more difficult for a hydrogen to be abstracted from this site, particularly at low temperatures, when compared to the primary site which has the lowest BDE and lowest propensity for low-temperature chain branching. The resultant fuel radical from primary hydrogen abstraction often instead produces an aldehyde and HO_2 radical from the first oxygen addition, drastically reducing reactivity.

While the 5-C surrogate proposed in this study produces an accurate representation of the reference gasoline's IDTs experimentally, the chosen model fails to fully predict this behavior, substantially underpredicting the intensity of the NTC region. This is matched by a further failure to replicate the LTHR behavior of the surrogate, as determined through the HRA of RCM pressure data. In the NTC region, measured pressure trace analysis shows two clear stages of LTHR, whereas simulations predict only a single stage. Sensitivity analyses at these same conditions identified 1-hexene and toluene oxidation species and reactions as highly sensitive. It is understood that both species play important roles in the development of LTHR and cool-flame phenomena, promoting and suppressing this behavior, respectively. When combined, these analyses indicate that the representation of LTHR behavior is essential for the accurate prediction of IDTs at these conditions. Therefore, this study proposes that HRRs (particularly in the LTHR and ITHR regions), as determined through the analysis of measured pressure traces from fundamental experiments (such as in an RCM), could serve as a useful target for future mechanism development. While little experimental data are currently available on this aspect of ignition delay studies, this study and others[54] have aimed to increase the data available and have shown that (while the process is nontrivial) the data can be extracted from existing RCM pressure traces. Mechanism development towards the reduction of model uncertainties would also benefit from the improvement of species thermodynamic data, through the reduction of individual GA group uncertainties and the application of experimental and quantum chemistry calculation methods to a wider range of species.

ACKNOWLEDGEMENTS

This research is supported by the EPSRC training grant: EP/L014912/1, regulated by the University of Leeds Centre for Doctoral Training in Bioenergy. Grateful acknowledgements are offered to Dr Scott Wagnon for his generous assistance in the development of the five component surrogate, Mark Batchelor, Samuel Flint, Peter Grieve, Dr Malcolm Lawes, and Dr Junfeng Yang for their assistance in the RCM lab and Prof. Derek Bradley and Dr Inna Gorbatenko for their valuable inputs. Also, thanks go to Roger Cracknell and Shell Global Solutions for the provision of the gasoline fuel, and Dr Mani Sarathy and the group at KAUST for providing the combined mechanism.

DATA AVAILABILITY STATEMENT

The data that supports the findings of this study are available within the article and the accompanying Supporting Information.

ORCID

Christian Michelbach https://orcid.org/0000-0001-6448-2705

REFERENCES

1. Sarathy SM, Oßwald P, Hansen N, Kohse-Höinghaus K. Alcohol combustion chemistry. *Prog Energy Combust Sci*. 2014;44:40-102.
2. Szwaja S, Naber JD. Combustion of *n*-butanol in a spark-ignition IC engine. *Fuel*. 2010;89 (7):1573-1582.
3. Wang C, Janssen A, Prakash A, Cracknell R, Xu H. Splash blended ethanol in a spark ignition engine – effect of RON, octane sensitivity and charge cooling. *Fuel*. 2017;196:21-31.
4. Nigam PS, Singh A. Production of liquid biofuels from renewable resources. *Prog Energy Combust Sci*. 2011;37(1):52-68.
5. Smith KM, Cho K-M, Liao JC. Engineering *Corynebacterium glutamicum* for isobutanol production. *Appl Microbiol Biotechnol*. 2010;87(3):1045-1055.
6. Weber BW, Sung C-J. Comparative autoignition trends in butanol isomers at elevated pressure. *Energy Fuels*. 2013;27(3):1688-1698.
7. Stranic I, Chase DP, Harmon JT, Yang S, Davidson DF, Hanson RK. Shock tube measurements of ignition delay times for the butanol isomers. *Combust Flame*. 2012;159(2):516-527.
8. Moss JT, Berkowitz AM, Oehlschlaeger MA, et al. An experimental and kinetic modeling study of the oxidation of the four isomers of butanol. *J Phys Chem A*. 2008;112(43):10843-10855.

9. McEnally CS, Pfefferle LD. Fuel Decomposition and hydrocarbon growth processes for oxygenated hydrocarbons: butyl alcohols. *Proc Combust Inst*. 2005;30(1):1363-1370.
10. Grana R, Frassoldati A, Faravelli T, et al. An experimental and kinetic modeling study of combustion of isomers of butanol. *Combust Flame*. 2010;157(11):2137-2154.
11. Gu X, Huang Z, Wu S, Li Q. Laminar burning velocities and flame instabilities of butanol isomers—air mixtures. *Combust Flame*. 2010;157 (12):2318-2325.
12. Veloo PS, Egolfopoulos FN. Flame propagation of butanol isomers/air mixtures. *Proc Combust Inst*. 2011;33(1):987-993.
13. Oßwald P, Güldenberg H, Kohse-Höinghaus K, Yang B, Yuan T, Qi F. Combustion of butanol isomers—a detailed molecular beam mass spectrometry investigation of their flame chemistry. *Combust Flame*. 2011;158(1):2-15.
14. Hansen N, Merchant SS, Harper MR, Green WH. The predictive capability of an automatically generated combustion chemistry mechanism: chemical structures of premixed iso-butanol flames. *Combust Flame*. 2013;160(11):2343-2351.
15. Pan L, Zhang Y, Tian Z, Yang F, Huang Z. Experimental and kinetic study on ignition delay times of *iso*-butanol. *Energy Fuels*. 2014;28(3):2160-2169.
16. Weber BW, Merchant S, Sung C-J, Green WH. An autoignition study of iso-butanol: experiments and modeling. *arXiv:170601827 [physics]*. 2013.
17. Wallington TJ, Kaiser EW, Farrell JT. Automotive fuels and internal combustion engines: a chemical perspective. *Chem Soc Rev*. 2006;35(4):335-347.
18. Sarathy SM, Farooq A, AlphaTIG GT. Recent progress in gasoline surrogate fuels. *Prog Energy Combust Sci*. 2018;65:67-108.
19. Curran HE, Pitz WJ, Westbrook CK, Callahan GV, Dryer FL. Oxidation of automotive primary reference fuels at elevated pressures. *Symp (Int) Combust*. 1998;27(1):379-387.
20. Westbrook CK, Pitz WJ, Mehl M, Curran HJ. Detailed chemical kinetic reaction mechanisms for primary reference fuels for diesel cetane number and spark-ignition octane number. *Proc Combust Inst*. 2011;33(1):185-192.
21. Park P, Keck JC. Rapid compression machine measurements of ignition delays for primary reference fuels. *SAE Trans*. 1990;99:11-23.
22. Kalghatgi G, Babiker H, Badra J. A simple method to predict knock using toluene, *n*-heptane and iso-octane blends (TPRF) as gasoline surrogates. *SAE Int J Engines*. 2015;8(2):505-519.
23. Cruz Da PA, Pera C, Anderlohr J, Bounaceur R, Battin-Leclerc F. A complex chemical kinetic mechanism for the oxidation of gasoline surrogate fuels: *n*-heptane, iso octane and toluene – mechanism development and validation. *arXiv:09034431 [physics]*. 2009.
24. Buda F, Bounaceur R, Warth V, Glaude PA, Fournet R, Battin-Leclerc F. Progress toward a unified detailed kinetic model for the autoignition of alkanes from C4 to C10 between 600 and 1200 K. *Combust Flame*. 2005;142(1):170-186.
25. Kukkadapu G, Kumar K, Sung C-J, Mehl M, Pitz WJ. Experimental and surrogate modeling study of gasoline ignition in a rapid compression machine. *Combust Flame*. 2012;159(10):3066-3078.
26. AlRamadan AS, Badra J, Javed T, et al. Mixed butanols addition to gasoline surrogates: shock tube ignition delay time measurements and chemical kinetic modeling. *Combust Flame*. 2015;162(10):3971-3979.
27. Gauthier BM, Davidson DF, Hanson RK. Shock tube determination of ignition delay times in full-blend and surrogate fuel mixtures. *Combust Flame*. 2004;139(4):300-311.
28. Gorbatenko I, Tomlin AS, Lawes M, Cracknell RF. Experimental and modelling study of the impacts of *n*-butanol blending on the auto-ignition behaviour of gasoline and its surrogate at low temperatures. *Proc Combust Inst*. 2019;37(1):501-509.
29. Agbro E, Tomlin AS, Lawes M, Park S, Sarathy SM. The influence of *n*-butanol blending on the ignition delay times of gasoline and its surrogate at high pressures. *Fuel*. 2017;187:211-219.
30. Lenhert DB, Miller DL, Cernansky NP, Owens KG. The oxidation of a gasoline surrogate in the negative temperature coefficient region. *Combust Flame*. 2009;156(3):549-564.
31. Kukkadapu G, Kumar K, Sung C-J, Mehl M, Pitz WJ. Autoignition of gasoline surrogates at low temperature combustion conditions. *Combust Flame*. 2015;162(5):2272-2285.
32. Fikri M, Herzler J, Starke R, Schulz C, Roth P, Kalghatgi GT. Autoignition of gasoline surrogates mixtures at intermediate temperatures and high pressures. *Combust Flame*. 2008;152(1):276-281.
33. Mehl M, Pitz WJ, Westbrook CK, Curran HJ. Kinetic modeling of gasoline surrogate components and mixtures under engine conditions. *Proc Combust Inst*. 2011;33(1):193-200.
34. Sarathy SM, Kukkadapu G, Mehl M, al. Ignition of alkane-rich FACE gasoline fuels and their surrogate mixtures. *Proc Combust Inst*. 2015;35(1):249-257.
35. Chen B, Togbé C, Wang Z, Dagaut P, Sarathy SM. Jet-stirred reactor oxidation of alkane-rich FACE gasoline fuels. *Proc Combust Inst*. 2017;36(1):517-524.
36. Sarathy SM, Kukkadapu G, Mehl M, et al. Compositional effects on the ignition of FACE gasolines. *Combust Flame*. 2016;169:171-193.
37. Hashimoto K, Koshi M, Miyoshi A, et al. *Development of Gasoline Combustion Reaction Model*. SAE Technical Paper 2013-01-0887. Warrendale, PA: SAE International; 2013.
38. Puduppakkam KV, Naik CV, Wang C, Meeks E. *Validation Studies of a Detailed Kinetics Mechanism for Diesel and Gasoline Surrogate Fuels*. SAE Technical Paper 2010-01-0545. Warrendale, PA: SAE International; 2010.
39. Andrae JCG. Development of a detailed kinetic model for gasoline surrogate fuels. *Fuel*. 2008;87(10):2013-2022.
40. Chung J, Lee S, An H, Song S, Chun KM. Rapid-compression machine studies on two-stage ignition characteristics of hydrocarbon autoignition and an investigation of new gasoline surrogates. *Energy*. 2015;93:1505-1514.
41. Agbro E, Zhang W, Tomlin AS, Burluka A. Experimental study on the influence of *n*-butanol blending on the combustion, autoignition, and knock properties of gasoline and its surrogate in a spark-ignition engine. *Energy Fuels*. 2018;32(10):10052-10064.
42. Sarathy SM, Vranckx S, Yasunaga K, et al. A comprehensive chemical kinetic combustion model for the four butanol isomers. *Combust Flame*. 2012;159(6):2028-2055.
43. Frassoldati A, Grana R, Faravelli T, Ranzi E, Oßwald P, Kohse-Höinghaus K. Detailed kinetic modeling of the combustion of the four butanol isomers in premixed low-pressure flames. *Combust Flame*. 2012;159(7):2295-2311.

44. Merchant SS, Zanoelo EF, Speth RL, Harper MR, Van Geem KM, Green WH. Combustion and pyrolysis of iso-butanol: experimental and chemical kinetic modeling study. *Combust Flame*. 2013;160(10):1907-1929.
45. Cai J, Yuan W, Ye L, et al. Experimental and kinetic modeling study of *i*-butanol pyrolysis and combustion. *Combust Flame*. 2014;161(8):1955-1971.
46. Cao J-R, Back MH. The heat of formation of the ethyl radical. *Int J Chem Kinet*. 1984;16(8):961-966.
47. Goldsmith CF, Magoon GR, Green WH. Database of small molecule thermochemistry for combustion. *J Phys Chem A*. 2012;116(36):9033-9057.
48. Olm C, Varga T, Valkó É, Hartl S, Hasse C, Turányi T. Development of an ethanol combustion mechanism based on a hierarchical optimization approach. *Int J Chem Kinet*. 2016;48(8):423-441.
49. Varga T, Olm C, Nagy T, et al. Development of a joint hydrogen and syngas combustion mechanism based on an optimization approach. *Int J Chem Kinet*. 2016;48(8):407-422.
50. Benson SW, Buss JH. Additivity rules for the estimation of molecular properties. Thermodynamic properties. *J Chem Phys*. 1958;29(3):546-572.
51. Hughes KJ, Griffiths JF, Fairweather M, Tomlin AS. Evaluation of models for the low temperature combustion of alkanes through interpretation of pressure–temperature ignition diagrams. *Phys Chem Chem Phys*. 2006;8(27):3197-3210.
52. vom Lehn F, Cai L, Pitsch H. Sensitivity analysis, uncertainty quantification, and optimization for thermochemical properties in chemical kinetic combustion models. *Proc Combust Inst*. 2019;37(1):771-779.
53. vom Lehn F, Cai L, Pitsch H, Thermochemical property estimation based on group additivity method: impact of groups on kinetic model predictions. In *Proceedings of the 9th European Combustion Meeting*, 2019.
54. Goldsborough SS, Santner J, Kang D, Fridlyand A, Rockstroh T, Jespersen MC. Heat release analysis for rapid compression machines: challenges and opportunities. *Proc Combust Inst*. 2019;37(1):603-611.
55. Curran H. A comprehensive modeling study of iso-octane oxidation. *Combust Flame*. 2002;129(3):253-280.
56. Curran HJ, Gaffuri P, Pitz WJ, Westbrook CK. A comprehensive modeling study of n-heptane oxidation. *Combust Flame*. 1998;114(1):149-177.
57. Park S, Wang Y, Chung SH, Sarathy SM. Compositional effects on PAH and soot formation in counterflow diffusion flames of gasoline surrogate fuels. *Combust Flame*. 2017;178:46-60.
58. Singh E, Badra J, Mehl M, Sarathy SM. Chemical kinetic insights into the octane number and octane sensitivity of gasoline surrogate mixtures. *Energy Fuels*. 2017;31(2):1945-1960.
59. Weber BW, Sung C-J, Renfro MW. On the uncertainty of temperature estimation in a rapid compression machine. *Combust Flame*. 2015;162(6):2518-2528.
60. Würmel J, Silke EJ, Curran HJ, Ó Conaire MS, Simmie JM. The effect of diluent gases on ignition delay times in the shock tube and in the rapid compression machine. *Combust Flame*. 2007;151(1–2):289-302.
61. Goodwin DG, Speth RL, Moffat HK, Weber BW. Cantera: An Object-Oriented Software Toolkit for Chemical Kinetics, Thermodynamics, and Transport Processes. 2018. https://doi.org/10.5281/zenodo.1174508.
62. Reaction Design. *CHEMKIN-PRO 15112*. San Diego, CA: Reaction Design; 2011.
63. Sung C-J, Curran HJ. Using rapid compression machines for chemical kinetics studies. *Prog Energy Combust Sci*. 2014;44:1-18.
64. Goldsborough SS, Hochgreb S, Vanhove G, Wooldridge MS, Curran HJ, Sung C-J. Advances in rapid compression machine studies of low- and intermediate-temperature autoignition phenomena. *Prog Energy Combust Sci*. 2017;63:1-78.
65. Mehl M, Wagnon S, Tsang K, et al, *A Comprehensive Detailed Kinetic Mechanism for the Simulation of Transportation Fuels*. Report LLNL-CONF-748072, 933145. Livermore, CA: Lawrence Livermore National Lab.; 2017.
66. Pelucchi M, Cai L, Pejpichestakul W, et al, computational chemistry consortium: surrogate fuel mechanism development, pollutants submechanisms and components library. Technical paper presented at 14th International Conference on Engines & Vehicles, Naples. 2019. https://doi.org/10.4271/2019-24-0020.
67. Seta T, Nakajima M, Miyoshi A. High-Temperature reactions of OH radicals with benzene and toluene. *J Phys Chem A*. 2006;110(15):5081-5090.
68. Reaction Design. *Reaction Workbench 15112*. San Diego, CA: Reaction Design; 2012.
69. Pepiot-Desjardins P, Pitsch H. An efficient error-propagation-based reduction method for large chemical kinetic mechanisms. *Combust Flame*. 2008;154(1):67-81.
70. Saylam A, Ribaucour M, Pitz WJ, Minetti R. Reduction of large detailed chemical kinetic mechanisms for autoignition using joint analyses of reaction rates and sensitivities. *Int J Chem Kinet*. 2007;39(4):181-196.
71. Minetti R, Ribaucour M, Carlier M, Fittschen C, Sochet LR. Experimental and modeling study of oxidation and autoignition of butane at high pressure. *Combust Flame*. 1994;96(3):201-211.
72. Reaction Design. ANSYS Chemkin-Pro 17.2 Theory Manual. 2016, 414.
73. Li S, Petzold L. Software and algorithms for sensitivity analysis of large-scale differential algebraic systems. *J Comput Appl Math*. 2000;125(1):131-145.
74. McBride BJ, Gordon S, Reno MA. Coefficients for calculating thermodynamic and transport properties of individual species. *NASA Tech Memo*. 1993:4513.
75. Goos E, Burcat A, Ruscic B. Extended Third Millennium Ideal Gas and Condensed Phase Thermochemical Database for Combustion with Updates from Active Thermochemical Tables. June 1, 2020.
76. Ruscic B. Uncertainty quantification in thermochemistry, benchmarking electronic structure computations, and Active Thermochemical Tables. *Int J Quantum Chem*. 2014;114(17):1097-1101.
77. Ruscic B, Pinzon RE, Laszewski G, et al. Active Thermochemical Tables: thermochemistry for the 21st century. *J Phys: Conf Ser*. 2005;16:561-570.
78. Mittal G, Bhari A. A rapid compression machine with crevice containment. *Combust Flame*. 2013;160(12):2975-2981.

79. Pilling MJ. *Low-Temperature Combustion and Autoignition*. New York, NY: Elsevier; 1997.
80. Vuilleumier D, Kozarac D, Mehl M, et al. Intermediate temperature heat release in an HCCI engine fueled by ethanol/*n*-heptane mixtures: an experimental and modeling study. *Combust Flame*. 2014;161(3):680-695.
81. Desgroux P, Minetti R, Sochet LR. Temperature distribution induced by pre-ignition reactions in a rapid compression machine. *Combust Sci Technol*. 1996;113(1):193-203.
82. Fridlyand A, Goldsborough SS, Al Rashidi M, Sarathy SM, Mehl M, Pitz WJ. Low temperature autoignition of 5-membered ring naphthenes: effects of substitution. *Combust Flame*. 2019;200:387-404.
83. Cheng S, Kang D, Fridlyand A, et al. Autoignition behavior of gasoline/ethanol blends at engine-relevant conditions. *Combust Flame*. 2020;216:369-384.
84. Atef N, Kukkadapu G, Mohamed SY, et al. A comprehensive iso-octane combustion model with improved thermochemistry and chemical kinetics. *Combust Flame*. 2017;178:111-134.
85. Zhang K, Banyon C, Togbé C, Dagaut P, Bugler J, Curran HJ. An experimental and kinetic modeling study of *n*-hexane oxidation. *Combust Flame*. 2015;162(11):4194-4207.
86. Bugler J, Marks B, Mathieu O, et al. An ignition delay time and chemical kinetic modeling study of the pentane isomers. *Combust Flame*. 2016;163:138-156.
87. Ellis C, Scott MS, Walker RW. Addition of toluene and ethylbenzene to mixtures of H_2 and O_2 at 772 K: Part 2: formation of products and determination of kinetic data for H+ additive and for other elementary reactions involved. *Combust Flame*. 2003;132(3):291-304.
88. Pelucchi M, Cavallotti C, Faravelli T, Klippenstein SJ. H-abstraction reactions by OH, HO_2, O, O_2 and benzyl radical addition to O_2 and their implications for kinetic modelling of toluene oxidation. *Phys Chem Chem Phys*. 2018;20(16):10607-10627.
89. da Silva G, Bozzelli JW. Kinetic modeling of the benzyl+HO_2 reaction. *Proc Combust Inst*. 2009;32(1):287-294.
90. Zhang K, Banyon C, Bugler J, et al. An updated experimental and kinetic modeling study of *n*-heptane oxidation. *Combust Flame*. 2016;172:116-135.
91. Burke SM, Simmie JM, Curran HJ. Critical evaluation of thermochemical properties of C1–C4 species: updated group-contributions to estimate thermochemical properties. *J Phys Chem Ref Data*. 2015;44(1):013101.
92. Bugler J, Somers KP, Silke EJ, Curran HJ. Revisiting the kinetics and thermodynamics of the low-temperature oxidation pathways of alkanes: a case study of the three pentane isomers. *J Phys Chem A*. 2015;119(28):7510-7527.
93. Tajti A, Szalay PG, Császár AG, et al. HEAT: high accuracy extrapolated *ab initio* thermochemistry. *J Chem Phys*. 2004;121(23):11599-11613.
94. Brown PN, Hindmarsh AC, Petzold LR. Using krylov methods in the solution of large-scale differential-algebraic systems. *SIAM Journal on Scientific Computing*. 1994;15(6):1467–1488. http://doi.org/10.1137/0915088.

SUPPORTING INFORMATION

Additional supporting information may be found online in the Supporting Information section at the end of the article.

How to cite this article: Michelbach C, Tomlin A. An experimental and kinetic modeling study of the ignition delay and heat release characteristics of a five component gasoline surrogate and its blends with iso-butanol within a rapid compression machine. *Int J Chem Kinet*. 2021;53:787–808. https://doi.org/10.1002/kin.21483